Annals of Biomedical Engineering, Vol. 40, No. 2, February 2012 (© 2012) pp. 304–331
DOI: 10.1007/s10439-011-0495-y

Fluorescence Lifetime Techniques in Medical Applications

LAURA MARCU

Department of Biomedical Engineering, University of California Davis, 451 Health Sciences Dr., Davis, CA 95616, USA

(*Received 17 September 2011; accepted 17 December 2011; published online 25 January 2012*)

Associate Editor Daniel Elson oversaw the review of this article.

Abstract—This article presents an overview of time-resolved (lifetime) fluorescence techniques used in biomedical diagnostics. In particular, we review the development of time-resolved fluorescence spectroscopy (TRFS) and fluorescence lifetime imaging (FLIM) instrumentation and associated methodologies which allow *in vivo* characterization and diagnosis of biological tissues. Emphasis is placed on the translational research potential of these techniques and on evaluating whether intrinsic fluorescence signals provide useful contrast for the diagnosis of human diseases including cancer (gastrointestinal tract, lung, head and neck, and brain), skin and eye diseases, and atherosclerotic cardiovascular disease.

Keywords—Time-resolved fluorescence spectroscopy and imaging, Medical applications of optical technologies, Tissue diagnosis *in vivo*.

FLUORESCENCE CONTRAST IN TISSUE

Fluorescence represents a ubiquitous means of achieving optical molecular contrast using diverse instruments including spectrophotometers, microarrays, microscopes, and endoscopes. Fluorescence measurements can provide information not only on the specific molecular makeup of a sample but also on the local environment surrounding the fluorescence molecule or fluorophore. Distinct species of fluorophores are characterized based on their excitation and emission spectra, their quantum efficiency, their polarization and their fluorescence lifetime.[28,61,84,99,125] Most common endogenous fluorophores in biological tissue used for tissue characterization include aromatic amino acids (tyrosine, tryptophane, and phenylalanine), structural proteins (elastin, collagens and collagen cross-links), enzyme metabolic co-factors [nicotinamide adenine (phosphate) dinucleotide (NAD(P)H) and flavin adenine dinucleotide (FAD)], lipid components and porphyrins. The absorption and emission characteristics of these fluorophores have been extensively studied and reviewed in numerous publications.[8,17,28,61,84,99,125] Alternatively, fluorescence measurements in tissue can take advantage of a broad range of exogenous molecular probes[8,54] with well-defined fluorescent characteristics. This includes a few probes approved for human use by the U.S. Food and Drug Administration (FDA) such as fluorescein and indocyanine green (ICG)[8,54] and porphyrin-based photosensitizers used in phototherapy.[1,27,41,95,103,110] This article focuses primarily on the use of tissue autofluorescence contrast as means of *in vivo* tissue characterization and diagnosis.

FLUORESCENCE IN TISSUE CHARACTERIZATION AND DIAGNOSIS

For a long time the measurement of tissue autofluorescence has being used as a means for the investigation of the molecular properties of biological cells and tissue as it has the potential to infer information about biochemical, functional and structural transformations of fluorescent bio-molecular complexes in these biological entities. Since such transformations can occur as a result of pathological transformation, therapeutic intervention[1,9,17,20,22,28,41,61,84,99,125] or during development,[5,32,37,97] fluorescence has been increasingly explored as a tool for tissue diagnosis. Moreover, the advances in light delivery and collection systems *via* fiber optics have facilitated the development of fluorescence-based techniques for non- or minimally invasive, remote investigations of tissues using endoscopic or catheter systems compatible with clinical application.[123] A wide range of applications of

Address correspondence to Laura Marcu, Department of Biomedical Engineering, University of California Davis, 451 Health Sciences Dr., Davis, CA 95616, USA. Electronic mail: lmarcu@ucdavis.edu

fluorescence techniques to tissue diagnostic, ranging from a variety of cancers to cardiovascular diseases and bioengineered tissues, were reported and presented in several pertinent publications.[1,5,8,9,17,20,22,28,32,37,84,97,99,125] Example of representative reviews of fluorescence-based studies in medicine include those by Wagnieres *et al.*,[125] Bigio and Mourant,[9] Andersson-Engels *et al.*,[1] Richards-Kortum and Sevick-Muraca,[99] Marcu,[68] and Ramanujam.[97]

Autofluorescence based contrast has been of particular interest in clinical research studies as the use of endogenous fluorescence for tissue characterization do not require the administration of a contrast agent. Both steady-state (intensity and/or spectrum) and time-resolved (time-domain or frequency-domain) fluorescence measurements (Fig. 1) have been employed for retrieving quantitative and qualitative information with respect to compositional makeup and pathophysiology of biological tissues. Table 1 presents a summary of the majority of autofluorescence studies[4,10–13,15,16,19,21,24–26,31,33–36,40,42,43,45,46,48,49,52,53,55,59,63,65,66,72–76,79,82,85,87,89–92,94,96,98,101,102,104,106–109,112,117,119,120,122,124,137–139] conducted *in vivo* in patients over the past 12 years. These studies have demonstrated the broad applicability of autofluorescence spectroscopy and imaging techniques for the diagnosis of tissue pathologies.

The steady-state technique, characterized typically by relative simple implementation and rather inexpensive instrumental setups, has been the most explored as a clinical tool for the diagnosis of diseased tissues *in vivo* in patients. In addition to experimental prototype systems engineered in individual research laboratories, commercial systems are nowadays available for autofluorescence measurements in tissues. For example, Xillix Technologies Corp (currently Novadaq Technologies Inc.),[128] Karl Storz,[129] Pentax,[130] and Richard Wolf[131] have commercialized such endoscopic systems LIFE, D-light, SAFE-100, and DAFE, respectively. These systems are equipped with a fluorescence excitation-collection module and designed to analyze autofluorescence contrast to diagnose cancers in the bronchi and gastrointestinal (GI) tract. Medispectra Inc. and SpectRx (currently Guided Therapeutics)[132] have developed devices incorporating fluorescence and reflectance spectroscopy for diagnosis of cancer of the cervix. Also, relatively recently the FDA has approved a new device VELscope (LED Dental, Inc.[133]) for direct visualization of autofluorescence of oral cavity and diagnosis of oral carcinoma. The reported sensitivity of many of these devices for detecting specific diseases stages is high, but their specificity remains limited.[14,84,122] This is due to a number of factors emerging from the difficulty to conduct absolute emission intensity measurements *in vivo*. The fluorescence intensity measurements are affected by changes in light excitation-collection geometries due to tissue movement, presence and change in concentration of endogenous absorbers (e.g., hemoglobin), potential non-uniform sample illumination due to variation in tissue surface profile, and photobleaching effects. To account for these limiting factors, in many situations the steady–state fluorescence measurements are accompanied by either diffuse reflectance spectroscopy (DRS) measurements in order to account for hemoglobin absorption or by rigorous calibration procedures designed to correct for potential

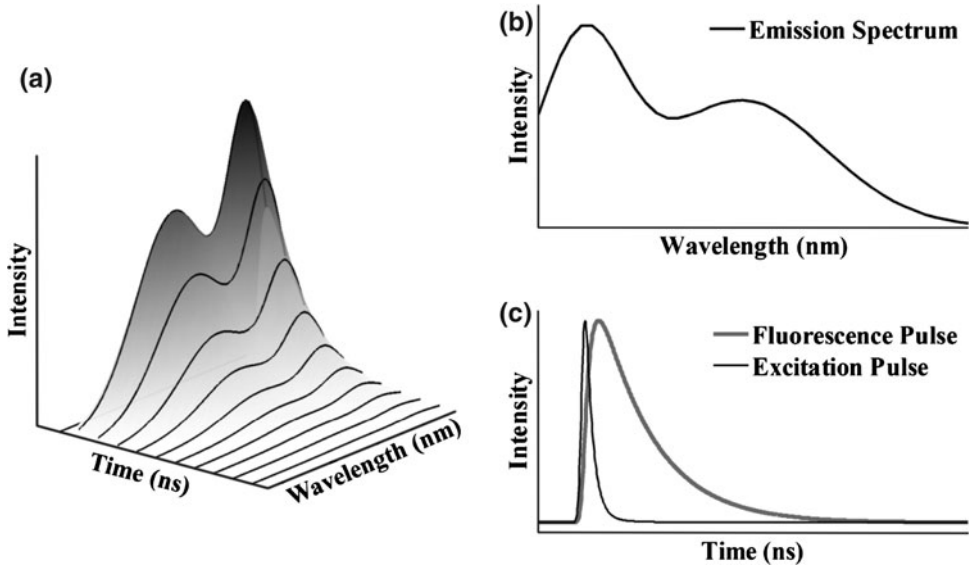

FIGURE 1. (a) Spectro-temporal profile of fluorescence emission in response to an excitation light stimuli; (b) Emission spectrum depicting the time-integrated intensities; (c) fluorescence pulse transient for a particular emission wavelength.

TABLE 1. Human *in vivo* studies for disease detection using endogenous fluorescence.

Anatomical site/organ	Method(s)	Excitation wavelength(s)/range/ bandwidth (nm)[c]	Emission wavelength/ bandwidth (nm)	Number of patients vs. measurements	Energy/ power	Examples of TRFS and FLIM characteristics	References
GI tract Esophagus Colon	SSFS endoscopic spectrometer and OMA	375–478	478–700	13	50 mW/cm^{2}[a]	NA	Mayinger *et al.*[76]
	SSFS endoscopic spectrometer and OMA	375–478	478–700	11/120	50 mW/cm^{2}[a]	NA	Mayinger *et al.*[75]
	SSF-IM and WLE endoscopic Filters and CCD	390–470	500–630	84	NA	NA	Curvers *et al.*[21]
	SSF-IM and WLE endoscopic	395–475	490–625	20/28	NA	NA	Kara *et al.*[52]
	SSF-IM and WLE endoscopic Filters and CCD	390–470	500–630	43	NA	NA	Suzuki *et al.*[117]
	TRFS Filters/APD, pulse sampling, digitizer, no deconvolution	337	550/40	17/4	0.5 μJ/pulse[b]	*Average decay time:* N: 10.5 ns D: 9.3 ns	Mycek *et al.*[85]
	TRFS and SSFS APD, pulse sampling, digitizer, spectrograph/ diode array, bi-exponential fitting	337/400	550/40	37/256	NA	*Parameters:* τ_1, τ_2, F_1 N: 1.46 ns, 6.50 ns, 0.47 D: 1.03 ns, 5.91 ns, 0.57	Pfefer *et al.*[92]
Lung/bronchi Larynx	SSFS & IM and DRS endoscopy Spectrograph/Camera	400–460	470–700	40/60	50 mW[a]	NA	Fawzy *et al.*[31]
	SSF-IM and WLB bronchoscopy SAFE-1000 system	420–480	490–590	123	NA	NA	Hanibuchi *et al.*[43]
	SSFS (modified bronchoscope) Fiber based spectrograph/CCD	350–495	400–800	48/1900	15 μW[a]	NA	Zellweger *et al.*[137]
	SSFS (modified bronchoscope) Fiber based spectrograph/CCD	350–480	400–800	48	9.2–24.4 μW[a]	NA	Zellweger *et al.*[138]
	SSFS (modified bronchoscope) spectrometer and CCD linear array, DAFE system	385–465	480–580	9	1.5 mW[a]	NA	Huttenberger *et al.*[49]
	SSF-IM and WLB bronchoscopy LIFE vs. D-light systems	Broad UV	400–600	332	NA	NA	Herth *et al.*[46]
	SSF-IM and WLB bronchoscopy Fiber based spectrograph/CCD	350–480	400–600	20	120 mW[a]	NA	Goujon *et al.*[40]
	SSF-IM with BRL modified DAFE system	430 $\pm$ 80	450–680	41	120 mW[a]	NA	Gabrecht *et al.*[34]

TABLE 1. Continued.

Anatomical site/organ	Method(s)	Excitation wavelength(s)/range/ bandwidth (nm)[c]	Emission wavelength/ bandwidth (nm)	Number of patients vs. measurements	Energy/ power	Examples of TRFS and FLIM characteristics	References
	SSF-IM and WLB with BRL DAFE system	430 ± 80	475–650	N/A	25 mW/cm^{2}[b]	NA	Gabrecht *et al.*[35]
	SSF-IM and WLB with BVL DAFE system	430 ± 80	410 and 490	12	NA	NA	Gabrecht *et al.*[36]
	SSF-microImaging (confocal) Cellvizio system	488	520–720	41	NA	NA	Thiberville *et al.*[119]
	TRFS and SSF-IM and WLB Spectrograph, streak camera, multi-exponential fit	405	430–680	11	NA	*Parameters:* τ_1, τ_2, τ_3: N: 0.17 ns, 2.02 ns, 6.84 ns; D: N /A, 2 ns, 7 ns	Uehlinger *et al.*[122]
	SSFS & IM OMA and D-light system	375–440	475–630	42	NA	NA	Arens *et al.*[4]
	SSFS & IM and WLL LIFE system	442	520/630	16/24	15–30 mV[a]	NA	Delank *et al.*[24]
GI: oral cavity	SSFS Spectrograph, CCD	350	400–560	3	NA	NA	Pavlova *et al.*[91]
	SSFS and DRS Spectrograph, CCD	300–470	390–650	124/424	NA	NA	Schwarz *et al.*[106]
	SSFS and DRS Spectrograph, CCD	350	400–560	NA/298	NA	NA	Pavlova *et al.*[90]
	SSFS Fiber optic and spectrofluorometer	300–360	350–600	40	NA	NA	Vedeswari *et al.*[124]
	SSFS and DRS and LSS Fiber optic and FastEEM	337–610	350–600	15/91	NA	NA	Muller *et al.*[82]
	SSFS and DRS Fiber optic and EEM	350–500	350–750	20/62 59/281	NA	NA	Heintzelman *et al.*[45]
	SSFS Fiber optic and spectrometer	337	370–700	144/477	50 μJ/pulse[b]	NA	Chaturvedi *et al.*[15]
	MDM and R-IM (wide-field imaging) Filters and CCD	365–450	410–600	N/A	2–12 mW/cm^{2}[b]	NA	Roblyer *et al.*[102]
	MDM and R-IM (wide-field imaging) Filters and CCD	365–450	410–600	67/276	NA	NA	Roblyer *et al.*[101]

TABLE 1. Continued.

Anatomical site/organ	Method(s)	Excitation wavelength(s)/range/ bandwidth (nm)[c]	Emission wavelength/ bandwidth (nm)	Number of patients vs. measurements	Energy/ power	Examples of TRFS and FLIM characteristics	References
	Fluorescence visualization Excitation and emission filters, eye	425	475	41	NA	NA	Lane *et al.*[63]
	TRFS Fiber optic, TCSPC, PMT, bi-exponential fit	410	633	55/76	N/A	*Averaged lifetime* N: ~6 ns D: ~10 to 12 ns	Chen *et al.*[16]
	TRFS and SSFS Monochromator, pulse sampling, digitizer, Laguerre deconvolution method	337	360–610	9/53	2 μJ/pulse[a]	*Averaged lifetime (390 vs. 460 nm emission)* N: ~ 1.47/1.5 ns D: ~ 1.38/1.38 ns	Meier *et al.*[79]
Cervix	SSFS and DRS Scanning and video system MediSpectra	337	360–600	604	22 μJ	NA	Huh *et al.*[48]
	SSFS and DRS Imaging spectrograph and camera	355	390–690	41/490	NA	N/A	Nordstrom *et al.*[87]
	SSFS and DRS Spectrograph/CCD and EEM	300–530	>350	330/748	N/A	N/A	Redden Weber *et al.*[98]
	SSFS and DRS Fiber optic and FastEEM	300–480	>350	850/3612	N/A	NA	Freeberg *et al.*[33]
Breast	SSFS and DRS Imaging spectrometer, CCD	337	360–650	40/179	45 μJ/pulse	N/A	Keller *et al.*[53]
	SSFS and DRS Imaging spectrometer, CCD, and EEM	300–400	350–600	73	NA	N/A	Zhu *et al.*[139]
Brain	SSFS and DRS Spectrograph and CCD	337	350–750	24	45 μJ/pulse[b]	NA	Toms *et al.*[120]
	SSFS and DRS Spectrograph and CCD	337	350–800	90	N/A	N/A	Lin *et al.*[65]
	SSFS Spectrograph and OMA	366	450–650	12	N/A	N/A	Croce *et al.*[19]
	SSFS and DRS Spectrograph and CCD	337	400–800	26/120	45 μJ/pulse[b]	NA	Lin *et al.*[66]
	FLIM Filters, gated ICCD, Laguerre deconvolution method	337	460 ± 25	3/13	0.16 mJ/cm^{2}[b]	*Averaged lifetime* N Cortex: ~1.28 ns High grade glioma: ~1.59 ns	Sun *et al.*[112]

TABLE 1. Continued.

Anatomical site/organ	Method(s)	Excitation wavelength(s)/range/ bandwidth (nm)[c]	Emission wavelength/ bandwidth (nm)	Number of patients vs. measurements	Energy/ power	Examples of TRFS and FLIM characteristics	References
	TRFS and SSFS Monochromator, PMT, pulse sampling, digitizer	337	360–550	17/123	3.0 μJ/pulse[a]	*Multiple conditions/ parameters*	Butte *et al.*[12]
	TRFS and SSFS Monochromator, PMT, pulse sampling, digitizer, Laguerre deconvolution method	337	360–550	42/186	3.0 μJ/pulse[a]	*Multiple conditions/ parameters*	Butte *et al.*[13]
Skin	SSFS and DRS Monochromator and PMT	295/350	400–600	18	50 μW/cm^{2}[b]	NA	Brancaleon *et al.*[11]
	SSFS Spectrograph, OMA	410	430–716	49	20 μJ/pulse[a]	N/A	Panjehpour *et al.*[89]
	SSFS and DRS Monochromator and PMT	337/445	350–700	40/48	NA	N/A	Rajaram *et al.*[96]
	CFM and MPM xy-scanner	780	400–700	1	125–187 pJ/pulse[a]	NA	Masters *et al.*[73]
	MP Microendoscopy GRIN lens, xy-scanner, DermaInspect	750–850	400–480	N/A	25 pJ/pulse[a]	N/A	Konig *et al.*[59]
	MP Tomography xy-scanner, DermaInspect	750–850	450	115	5–35 mW[b]	N/A	Dimitrow *et al.*[26]
	MP Tomography and SHG DermaInspect	820	410/470	18	49 mW (laser power)	NA	Koehler *et al.*[55]
	MP Tomography and spectral FLIM DermaInspect with TCSPC module, bi-exponential fit	760/800	380–580	23/46	5–50 mW (laser power)	*Multiple conditions/ parameters*	Dimitrow *et al.*[25]
	MP-FLIM and MP-SSFS Frequency-domain (80 MHz), xy-scanner, PMT	730/960	425/520	1	10–15 mW[b]	*Normal skin:* $\tau_{phase} = 0.5$ ns, $\tau_{mod} = 1.7$ ns.	Masters *et al.*[74]
	TRFS TCSPC, Monochromator Multi-exponential fit	375	442/460/478/496	75	2.07×10^{-6} W/cm^{2} μW/pulse[b]	*Multiple conditions/ parameters*	Blackwell *et al.*[10]
	TRFS and SSFS Pulse sampling, digitizer Spectrograph and ICCD, bi-exponential fit	337	460	N/A	20 μJ/pulse (laser power)	*Parameters:* τ_1, τ_2, F_1 Normal skin: 0.9 ns, 5.3 ns, 0.40	Pitts *et al.*[94]

TABLE 1. Continued.

Anatomical site/organ	Method(s)	Excitation wavelength(s)/range/ bandwidth (nm)[c]	Emission wavelength/ bandwidth (nm)	Number of patients vs. measurements	Energy/ power	Examples of TRFS and FLIM characteristics	References
Eye	SSF-IM (Wide-field) Filters and CCD	475–515 476–604	530–675 675–715	78	NA	NA	Hammer *et al.*[42]
	FLIM TCSPC, xy-scanner, Multi-exponential fit	446	>475	6	60 μW[b]	*Parameters:* τ_1, τ_2 Normal optic disk: 0.5–1.5, 2–5 ns	Schweitzer *et al.*[107]
	FLIM TCSPC, xy-scanner Multi-exponential fit	448	490–560 560–700	6	120 μW	*Multiple conditions/parameters*	Schweitzer *et al.*[109]
	FLIM TCSPC, xy-scanner, Multi-exponential fit	448	490–560 560–700	23	NA	*Multiple conditions/parameters*	Schweitzer *et al.*[108]
Arteries	SFS, DRS, Raman spectroscopy Spectrograph and CCD	337	370–640	12	4 μJ/pulse	NA	Scepanovic *et al.*[104]
	TRFS and SSFS Monochromator, pulse sampling, digitizer, Laguerre deconvolution method	337	360–550	65	2 μJ/pulse	*Multiple conditions/parameters*	Marcu *et al.*[72]

APD, Avalanche photodiode; BRF, Backscatter red light; BVL, Backscatter ultraviolet light; CCD, Charge-coupled detector; CFM, Confocal microscopy; DRS, Diffuse reflectance spectroscopy; EEM, Excitation emission matrix; FLIM, Fluorescence lifetime imaging microscopy; GRIN, Gradient Index; ICCD, Intensified charge-coupled detector; LSS, Light scattering spectroscopy; MDM, Multispectral digital microscopy; MP, Multiphoton; MPM, Multiphoton Microscopy; OMA, Optical Multichannel Analyzer; PMT, Photomultiplier; R-IM, Reflectance imaging; SHG, Second Harmonic Generation; SSFS, Steady-state (intensity-based) fluorescence spectroscopy; SSF-IM, Steady-state ((intensity-based) fluorescence imaging; TCSPC, Time-correlated single photon counting; TRFS, Time-resolved fluorescence spectroscopy; WLB, White light bronchoscopy; WLE, White light endoscopy; WLL, White light laryngology; N, Normal (healthy) tissue; D, Diseased tissue.

Fluorescence decay parameters (multi-exponential fitting): τ_1, τ_2, τ_3 (time constants); F_1, F_2, F_3 (fractional contributions).

[a]Denotes the energy/power at the distal end of the illumination fiber-optic or fiber-bundle.

[b]Denotes the energy/power at tissue level.

[c]Denotes the wavelength-range (broad UV spectrum) used for tissue excitation.

factors that non-linear affect the measured fluorescence intensity values.[11,31,33,48,53,65,66,72,82,87,90,96,98,106,120,139]

The alternative method to measure fluorescence, time-resolved (lifetime) technique, can address the limitations of the steady-state technique by resolving the dynamics of fluorescence decay; thus capitalizing on the additional dimension of fluorescence emission—the excited state lifetime(s). This approach also improves the specificity of fluorescence measurements.[8,17,28,99] Conceptually, the fluorescence lifetime is the average time a fluorophore spends in the excited states following excitation from its ground energy level. As many of the fluorophores in biological tissues have an overlapping spectra,[17,84,125] the fluorescence lifetime properties can provide a contrast parameter. Also, the fluorescence lifetime varies with the molecular environment (e.g., pH, pO_2 values) and the fluorescence decay time is usually independent of fluorophore concentration and its quantum yield.[17,28,61] In brief, the use of time-resolved fluorescence for studying biological systems offers several distinct advantages including a means: (a) to resolve biomolecules with overlapping fluorescence emission spectra but with different fluorescence decay times; (b) to account for quenching of the fluorescence by change of the physicochemical environment as the measurements are sensitive to various parameters of the biological microenvironment (including pH, ion concentration and binding, enzymatic activity, temperature, redox state); (c) for more robust quantitative measurements *in vivo* since the lifetime measurements are independent of intensity.

Despite these recognized inherent advantages, the full potential value of fluorescence lifetime information has not been extensively evaluated in clinical settings due to several barriers. This includes the complexity of the instrumental setup, the lengthy data acquisition and analysis, and the high instrumentation cost. As clearly demonstrated by the listing of reports depicted in Table 1 only a fraction of the total clinical research studies in patients *in vivo* are based on time-resolved techniques. Numerous time-resolved fluorescence studies were conducted in excised tissue specimens,[17,20,22,28,68,84] however the outcome of these studies cannot be fully extrapolated to *in vivo* measurements.[68,71,72] This is due to changes in tissue biochemical composition related to functional properties (e.g., metabolism, hypoxia, *etc.*) as well as changes in tissue morphology generated by shrinkage or other factors that affect tissue geometry post-excision. Consequently, motivated by an increased interest in identifying enabling solutions for the development of fluorescence lifetime-based instrumentation suitable for clinical applications, this article focuses on reviewing the use of time-resolved fluorescence techniques (both point spectroscopy and lifetime imaging) for label-free characterization and diagnosis of tissue pathologies in human patients *in vivo*; and on indentifying challenges that hamper a broader translation of these techniques to clinical settings.

OVERVIEW OF TIME-RESOLVED FLUORESCENCE SPECTROSCOPY AND IMAGING TECHNIQUES

Fluorescence lifetime (time-resolved) measurements can be conducted in either the time-domain or frequency-domain. Both approaches provide equivalent information about the decay of fluorescence intensity. However, there are considerable differences in the implementation and applications of these two approaches. In the following we present a brief description of the principle behind the time-domain techniques primarily used for *in vivo* tissue investigations; specifically time-correlated single-photon counting (TCSPC) and pulse sampling and gated detection (Figs. 2a, 2b, 2c). For reference, we also describe the principle of the frequency-domain method (Fig. 2d).

Moreover, in practice fluorescence lifetime information from biological tissue is determined through either spectroscopy systems for point measurements (single channel) or imaging spectroscopy (multiple channels) systems. The latter also is known also as fluorescence lifetime imaging microscopy (FLIM). A comprehensive overview of point spectroscopy and FLIM techniques, both scanning and wide-field, and their potential applications have been extensively reviewed in previous publications.[8,20,28,61]

Principles of Time-Resolved Techniques Used in Tissue Characterization

The time-resolved time-domain approach relies on instrumentation that measures the fluorescence emission as a function of time delay following pulsed excitation.[20,22,28,61] TCSPC is the most commonly used technique for time-resolved measurements in both point spectroscopy and imaging systems.[61] This technique has been not only extensively described in the literature[8,20,28,61] but also implemented in general purposes commercial fluorescence lifetime systems such those developed by PicoQuant GmbH[135] and Becker and Hickl GmbH.[136] TCSPC has been generally preferred for fluorescence lifetime measurements due to its high sensitivity and low degree of systematic errors where the standard deviation of each measurement can be estimated from Poisson statistics. This is important in particular when the aim of the measurement is the resolution of complex intensity decay. In TCSPC the

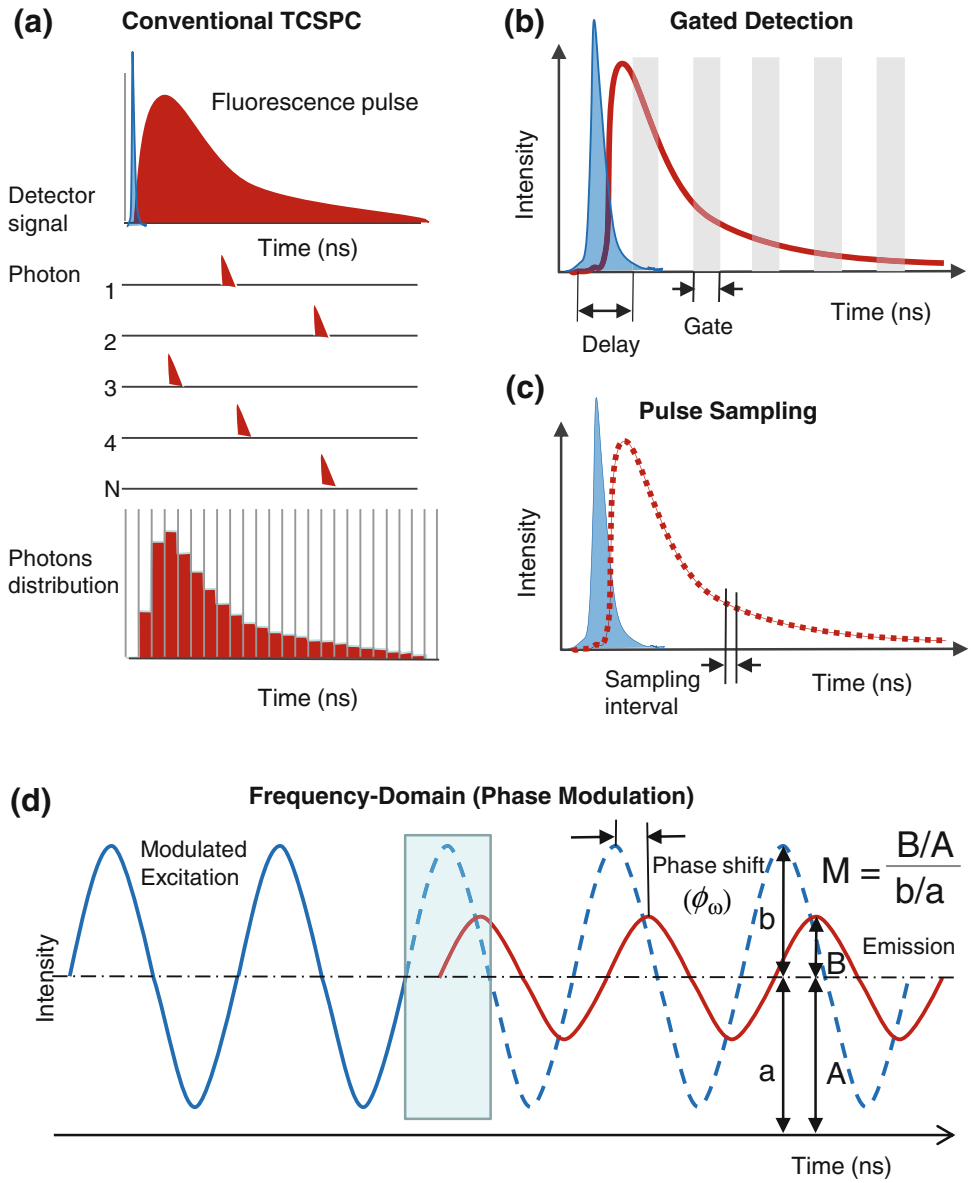

FIGURE 2. Schematic of principles behind the main types of time-resolved (lifetime) measurement methods. (a) Conventional TCSPS; (b) Gated detection using a gated detector (e.g., gated ICCD camera); (c) Pulse sampling using a digitizer working at a high sampling rate and analog bandwidth; and (d) Frequency-domain (phase-modulation). Parameter M represents the demodulation factor or ratio. The ratios B/A and b/a represent the modulation of the emission and excitation, respectively. Schematics adapted from Lakowicz.[61]

sample is excited by a pulse train of light and the emitted photons are recorded in a manner that at low emission fluxes a histogram of photon arrival time is build-up (Fig. 2a). This is achieved through recording a series of voltage signals that depend on the arrival time of individual detected photons relative to the excitation pulse. With a high repetition rate laser light source the fluorescence pulse response can be recorded in a short time. The resulting histogram counts vs. channels represent the change of fluorescence intensity vs. time. If a system for sample scanning is used, spatial information from the scanning electronics, a fluorescence lifetime images can be acquired. This represents a direct way to implement FLIM on conventional scanning microscopes.[28,58,60] Overall, this technique has played an important role for the development of both point spectroscopy (TRFS) and imaging (FLIM) systems.

More recently, an alternative technique, pulse sampling and gated detection, has become popular in tissue diagnosis owing to recent advances in fast electronics and detectors. This technique can be implemented in two ways.[61] In the first approach (Fig. 2b), a time-gated detector is used. In this case, a train of finite excitation pulses are used to induce the fluorescence

emission of the sample. The fluorescence intensities at each distinct delay time along the decay curve are integrated by the detector and used to reconstruct the decay curve (intensity vs. time). Typically, a time-gated intensified charge-coupled device (ICCD) is employed for such measurement. This detection technique is preferred in wide-field FLIM.[28,77] In the second approach (Fig. 2c), the detector is kept on until the entire fluorescence transient pulse is detected. If the sample quantum efficiency is high enough (above the detection system noise level) a single excitation pulse suffices in order to record a transient response pulse. The resulting electrical pulse signal is subsequently sampled using a digitizer (e.g., digital oscilloscope) with high sampling frequency and analog bandwidth (resolution of tens of picoseconds). The second detection method has been used by several groups for point spectroscopy TRFS[12,13,72,79,85,92,94] and more recently scanning FLIM.[111] Given its ability to rapidly collect fluorescence decays, this latter method is suitable for clinical applications. A constraint of this method, however, is the lack of information on the nature of the instrument noise. This may lead to the introduction of systematic error that could hamper an accurate recovery of the fluorescence decay. Overall, the TCSPC technique (single-photon) is characterized by high sensitivity and high temporal resolution but slow data acquisition. In contrast, the time-gated detection is characterized by fast and simultaneous acquisition of all pixels (i.e., FLIM), but lower sensitivity, and also requires a moderate sample fluorescence emission.

The time-domain technique requires complex opto-electronic equipment that challenges its clinical implementation. Typically, this technique involves fast wide-field (cameras) and point (photomultipliers) detectors for fluorescence detection and ps- and fs-pulsed lasers for fluorescence excitation. Also, there are limited options for pulsed lasers in UV range (330–400 nm) corresponding to the absorption spectra of the majority of endogenous fluorophores. The time-domain systems, however, present some unique advantages.[20] For example the Fourier spectrum of a short laser pulse is broad enough to provide a wide band stimulus that allows complex fluorescence decay dynamics (multiple lifetimes) to be measured at once. In addition, pulsed laser systems working at low repetition rate (<10 kHz) do not require complete darkness and can be operated at room light, which make them compatible with clinical environment.[20] Time-domain techniques based on both single- and multiphoton-excitation[58,100] have been used for tissue fluorophores excitation. The latter approach carries specific advantages including the availability of high repetition rate and tunable pulsed lasers in near infrared (NIR) range. This type of lasers not only provides a broad range of tissue excitation wavelengths but also the use of NIR light for tissue excitation decreases the global tissue phototoxicity and improves the penetration depth. The technical complexity of multi-photon based instrumentation, however, has limited the use of this approach to sites that can be easily exposed to light excitation (e.g., skin). In fact, the only clinical diagnostic commercial system DermaInspect (JenLab GmbH)[58,134] incorporating a time-resolved fluorescence measurement module is used for detection of dermatologic disorders.

The frequency-domain technique relies in an intensity-modulated excitation light source (Fig. 2d). This technique derives the lifetime information from measurements of phase difference ($\varnothing_\omega$) between a sinusoidally modulated excitation and the resulting sinusoidally modulated fluorescence signal, where ω is the modulation frequency in radians/s. In addition, the finite response of the sample results in demodulation of the emission as defined by the demodulation factor M.[20,22,28,61] In tissue studies, the frequency-domain detection was initially preferred due to the relatively simpler electronic instrumentation and excitation source requirements. Nevertheless, measurements of complex intensity decay require repeated experiments at different excitation modulation frequency in order to take into account the entire fluorescence decay dynamics.[20,61] This results in increased data acquisition and analysis time which has limited the suitability of this approach for clinical applications.

Time-Resolved Fluorescence—Data Analysis Methods

The fluorescence intensity decay profiles resulting from time-resolved measurements of tissues are often complex. Tissue endogenous fluorophore are characterized by a broad and overlapping absorption spectrum, thus typically more than one fluorophore are excited simultaneously. The measured fluorescence decay represents the superposition of all individual decay components that cannot be fit by a single-exponential decay model. In addition, the shape of the measured fluorescent pulse transient is affected by the optical and electronic components of the instrumental apparatus. Mathematically, the measured fluorescence intensity decay is the convolution of the fluorescence impulse response function (fIRF) with the instrument response. Thus, to estimate the fIRF of a sample, the instrument response must be deconvolved from the measured fluorescence pulse transient.[61,88,126] For example in the context of discrete TRFS or FLIM data, the measured fluorescence intensity decay data $y(n)$ is given by the convolution of the fIRF $h(n)$ with the instrument response $x(n)$:

$$y(n) = T \cdot \sum_{m=0}^{K-1} h(m)x(n-m), \quad n = 0, \ldots, N-1$$

The parameter K determines the length of the fluorescence decay (fIRF), N is the number of time samples recorded for both $y(n)$ and $x(n)$, and T is the sampling interval (time-resolution of the instrument). Methods for recovery fIRF from tissue fluorescence measurements would ideally encompass a way to best estimate the shape of florescence decay and a rapid method for deconvolution. In the following we briefly overview the most common methods used in the analysis of fluorescence decay from time-resolved measurement performed *in vivo* in human tissues.

The most regularly applied deconvolution method is the least-square iterative reconvolution (LSIR) in conjunction with a multi-exponential approximation of decay function[28,61,88,126]:

$$h(n) = \sum_{i=1}^{M} A_i e^{\left(\frac{n}{\tau_i}\right)}$$

where τ_i and A_i represent the decay times and the corresponding amplitude coefficients, respectively. This technique applies nonlinear least-square optimization methods (i.e., Gauss–Newton, Lavenberg–Marquardt) to estimate the parameters of a multi-exponential fIRF that would fit best its convolution with the system response to the fluorescence decay data. Since the optimization process involves iterative convolutions, LSIR is typically computationally expensive. Also, since exponential functions do not form an orthonormal basis, distinct multi-exponential terms can be fitted to a particular fluorescence decay profile. This is due to the correlation of the fitting parameters in the multi-exponential model. Also, as noted above the fluorescence emission in tissues originates from several endogenous fluorescent sources. Thus the origin of autofluorescence in a complex medium such as biological tissues is not fully understood and often there is no a priori knowledge of the fluorescence decay model. The analysis of time-resolved fluorescence decay in terms of multi-exponential components therefore is not entirely adequate. Such components often cannot be interpreted in terms of fluorophore content or number of discrete lifetimes components.[20,61] Thus there is an advantage in avoiding any a priori assumption about the functional form of the fIRF decay.

An alternative model-free deconvolution method for applied to fluorescence decay data analysis concerns expansion of the fIRF on a Laguerre basis of functions.[50,51,68] This approach was found to provide significant advantages over the more traditional methods when applied to tissue characterization. The method is based on the expansion of kernels (fIRF, for linear systems) on a set of orthonormal set of discrete time Laguerre functions (LF) $b_j^{\alpha}(n)$:

$$h(n) = \sum_{j=0}^{L-1} c_j b_j^{\alpha}(n)$$

In the equation above, c_j^{α} are the unknown Laguerre expansion coefficients (LEC), which are estimated from the input–output data; $b_j^{\alpha}(n)$ denotes the jth order ortho-normal discrete LF; L is the number of discrete LFs used to model the fIRF, thus defining the order of the expansion. The LF basis is defined as:

$$b_j^{\alpha}(n) = \alpha^{(n-j)/2}(1-\alpha)^{1/2} \sum_{k=0}^{j} (-1)^k \times \binom{n}{k}\binom{j}{k} \alpha^{j-k}(1-\alpha)^k, \quad n \geq 0$$

The functions of higher order converge slower to zero. The LF include a build-in exponential term, thus they are suitable for physical systems with asymptotically exponential relaxation dynamics. The Laguerre parameter α ($0 < \alpha < 1$) determines the rate of exponential (asymptotic) decline of the discrete LFs. The choice of the parameter α is important in achieving accurate fIRF estimations. In general, fIRF with longer lifetime would require larger values of α for efficient representation, and vice versa. In practice, the parameter α can be selected based on the length of $h(n)$ and the number of LFs used for the expansion, so that all functions converge to zero by the end of the fIRF. Alternatively, these parameters could be also iteratively optimized. Overall, the Laguerre approach does not require a priori knowledge of the fluorescence decay function and allows for fast converging kernel estimation from short input–output data records, using least-square estimation of the expansion coefficients. Because the Laguerre basis is a complete orthonormal set of functions, it can always provide a unique and complete expansion of the fluorescence dynamics (decay function). Moreover, it enables fast deconvolution of input from the output as it resumes to solving a linear least-square minimization problem. Also, the Laguerre coefficients (c_j) can be used in the characterization of the fluorescence system. This method was adapted and successfully applied to the deconvolution of fluorescence decay data from tissues measured *in vivo*.[12,13,68,72]

APPLICATIONS OF TIME-RESOLVED FLUORESCENCE TO DIAGNOSIS OF PATHOLOGIC CONDITIONS IN HUMANS

In the following we review the autofluorescence studies conducted in human patients *in vivo*. Emphasis is placed on the TRFS and FLIM techniques and their applications for (i) diagnosis of cancer of the GI tract,

bronchi/lung, skin, head and neck, and brain; (ii) ophthalmic pathologies; and (iii) atherosclerotic cardiovascular disease.

Cancer Diagnostics

Gastrointestinal tract (GI) and bronchi: Conventional clinical endoscopic devices such as the white light endoscopes (WLE), bronchoscopes (WLB) or laryngoscopes (WLL) along with the availability of commercial endoscopic fluorescence imaging (e.g., Xillis LIFE, Stortz D-Light, Pentax 3000, or Richard Wolf DAFE)[128–131] systems have enabled an extensive evaluation of autofluorescence as a tool for diagnosis of cancer in the GI tract (e.g., colonic polyps and Barrett's esophagus) and cancer in the bronchi and larynx. However, as shown above (Table 1) the majority of these studies were based on measurements of fluorescence intensity in either imaging or spectroscopy format. Generally, the lower fluorescence intensity values along with specific changes in spectral emission profile exhibited by tumor when compared with the surrounding normal tissue were used for the delineation of the diseased tissue. The fluorescence measurement, however, in most cases was combined with conventional white light imaging and backscatter light to improve the diagnostic accuracy of Barrett's esophagus[127] or lesions in the bronchi.[38,62] Only a limited number of studies[39,85,92,122] employed TRFS-based analysis of these tumors. These are described in the following.

Similar to the steady-state techniques, the evaluation of the time-resolved techniques in patients *in vivo* took advantage of existing clinical endoscopic systems. A fiber-optic probe introduced in the accessory port of the endoscope was typically used to access the tissue of interest. One of the first TRFS reports[85] concerns a pulse-sampling technique applied to the diagnosis of colonic polyps. The instrumental setup included fluorescence excitation *via* a pulsed nitrogen laser (337 nm, 4 ns, 20 Hz repetition rate) and detection *via* an avalanche photodiode and digital oscilloscope (500 MHz bandwidth, 2 GS/s sampling rate). This study targeted the discrimination of adenomatous and hyperplastic colonic polyps. Adenomatous polyps are a convenient model for dysplasia easily located and highly prevalent.[92] The study was conducted in 17 patients (total 24 polyps; 13 adenomatous, 11 non-adenomatous). The results of this study indicated that the autofluorescence emission decay (excitation 337 nm, emission 550 ± 20 nm bandpass) from adenomas was faster than that from non-adenomas polyps (Table 1). No deconvolution method was used for analysis of the dynamics of the fluorescence decay rather the fluorescent pulse width was evaluated. While no specific dysplasia signatures were determined, the authors reported that the measured decay time provided a means of distinguishing adenomas from non-adenomas with a sensitivity (proportion of patients with disease who test positive) of 85%, and specificity (proportion of patients with disease who test positive) of 91%. The use of a much larger data set (237 polyps) in a subsequent report[83] resulted in much lower levels of sensitivity and specificity (73 and 70%, respectively). Despite this successful application of TRFS to this site, few subsequent efforts have been made to extend the TRFS studies in this area.

Extending on the pulse-sampling TRFS instrumental setup described above, another study[92] reported the potential of this technique for diagnosis of high grade dysplasia in Barrett's esophagus (37 patients, 108 point measurements). The modified system allowed for the use of two excitation wavelengths (337 and 400 nm through the addition of a dye module to the nitrogen laser) and recording of fluorescence decay in 550 ± 20 wavelength range. Moreover, a spectrograph coupled to a diode array enabled simultaneous recording of the entire fluorescence emission spectrum, thus both wavelength- and time-resolved data were available for tissue characterization. The dynamics of the intensity decay was analyzed using a bi-exponential function. Although none of the parameters calculated from the time-resolved data permitted tissue classification with high accuracy, the individual decay trends for excitation at 337 nm demonstrate that the dysplastic tissue produces a faster decay than the non-dysplastic tissue (Table 1). This trend is similar to that obtained for the colonic polyps. However, no defined trends were obtained when tissue was excited at 400 nm. Overall in this study, the classification accuracy of spectrally resolved data alone was not improved by the addition of the time-resolved data.

A distinct TRFS instrumental setup for clinical tissue characterization during endoscopy was reported by Glanzmann *et al.*[39] This instrument uses also a nitrogen laser pumped-dye laser (repetition rate between 1 and 50 Hz) to excite the tissue fluorescence. However, it employs a spectrograph to resolve the sample emission and a streak camera placed in the image plane of the spectrograph to spectrally (640 channels) and temporally (480 channels) resolve the fluorescence emission. This fast two-dimensional detector provided means to fast resolve the decay of the entire fluorescence spectra with a high dynamic range (subnanoseconds-to-miliseconds). An example of such measurement is given in Fig. 3. The initial validation of this system was demonstrated for nine case *in vivo* florescence measurement (case studies) in the bronchi, oral cavity, esophagus, and bladder.[39]

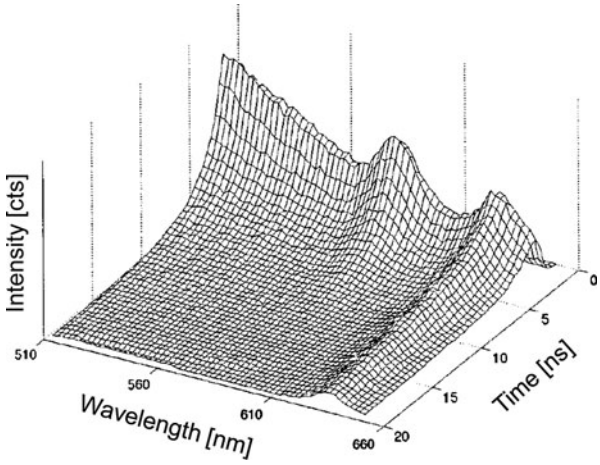

FIGURE 3. Example of a spectro-temporal fluorescence profile obtained using a streak camera placed in the plane of a spectrograph to spectrally and temporally resolve the fluorescence emission in multiple channels. Adapted from Glanzmann *et al.*[118] Courtesy: G. Wagnieres, Swiss Federal Institute of Technology.

The measurements were conducted in patients undergoing routine endoscopy for cancer screening or photodynamic therapy. A more extended validation of this technique in humans was reported in a later study[122] conducted in 11 lung cancer patients undergoing conventional WLB. Tissue autofluorescence was excited at 405 nm and the analysis of the fluorescence decay was based on multi-exponential decay function. Interestingly, the authors reported that although differences in the fluorescence (excited at 405 nm) decay parameters for distinct tissue conditions (preneoplastic, microinvasive neoplastic, and healthy mucosa in the bronchi) were found such differences are small in comparison to the inter- and intra-patient variations of the autofluorescence on healthy mucosa. The mucosa heterogeneities appeared to account for most of the changes of the lifetime(s) values. Despite the limited ability of lifetime data to finely discriminate distinct tissue pathologies, this study provided useful insights into the mechanisms underlying the autofluorescence spectral and intensity contrast in bronchial tissue.

Oral Carcinoma

The potential role of autofluorescence contrast as a means of diagnosis of head and neck tumors including the cancer of the oral cavity was also extensively evaluated *via* a variety of point spectroscopy and imaging techniques.[15,24,45,63,82,90,91,101,102,105,106,124] The relative direct accessibility of these tumor sites enabled the development of both point spectroscopy and wide-field imaging devices that can access the area of interest *via* flexible (fiber optic), semi-flexible (light guide), or rigid (direct illumination) light guides. The availability of the commercial device VELscope (LED Dental, Inc.)[133] has also enabled clinicians to directly visualize fluorescence in oral cavity. However, as for the cancer in the GI tract or bronchi the majority of devices tested in patients were based on steady-state spectroscopy techniques or intensity-based imaging. In order to improve the specificity of the fluorescence measurements the clinical device incorporated complementary diagnostic techniques such as diffuse reflectance spectroscopy[82,106] and light scattering spectroscopy,[82] depth sensitive probes,[105,106] advanced computational models of signal calibration, and digital imaging processing.[101] Only two reports[16,79] describe the use of TRFS point spectroscopy systems for characterization and diagnosis of oral carcinoma in patients. In both cases excitation and collection of the autofluorescence signal was achieved *via* customized handheld bifurcated fiber bundle probes.

The first study by Chen *et al.*[16] employed a commercial available TCSPC system (HORIBA Jobin–Yvon IBH) consisting of a pulsed laser diode (excitation at 408 nm, pulse width 70 ps (FWHM)), a fast response photomultiplier, and a single photon counting device to study the autofluorescence emission (633 nm) corresponding to the porphyrin fluorescence as a means to differentiate in 38 patients normal oral mucosa from oral premalignant lesions including verrucous hyperplasia epithelial hyperplasia, and epithelial dysplasia. The fluorescence decay was fitted with a biexponential model. The research findings demonstrated that the fluorescence of normal mucosa at 633 nm emission exhibits a significantly faster decay dynamics when compared with dysplastic tissue (Table 1) that enables a good discrimination of distinct pathologies.

The second study conducted by our research group employed two fluorescence lifetime systems (TRFS and FLIM devices) for characterizing the fluorescence of cancer located on buccal mucosa, tongue, vocal cord and floor of the mouth. A subset of results from these studies was recently reported.[79,116] Nine patients with suspected head and neck squamous cell carcinoma (HNSCC) were enrolled in intraoperative studies. TRFS data was recorded from 53 locations while FLIM images were acquired from 26 areas. For the TRFS we employed a pulse-sampling apparatus (Fig. 4) similar to that that reported earlier by our research group.[30,113] This apparatus entails fluorescence excitation *via* a pulsed nitrogen laser (excitation at 337 nm, pulse width 700 ps (FWHM), 30 Hz repetition rate) and detection *via* a gated MCP-PMT and digital oscilloscope (2.5 GHz bandwidth, 40 GS/s sampling rate). A scanning monochromator allowed for sequential acquisition (360–610 nm spectral range,

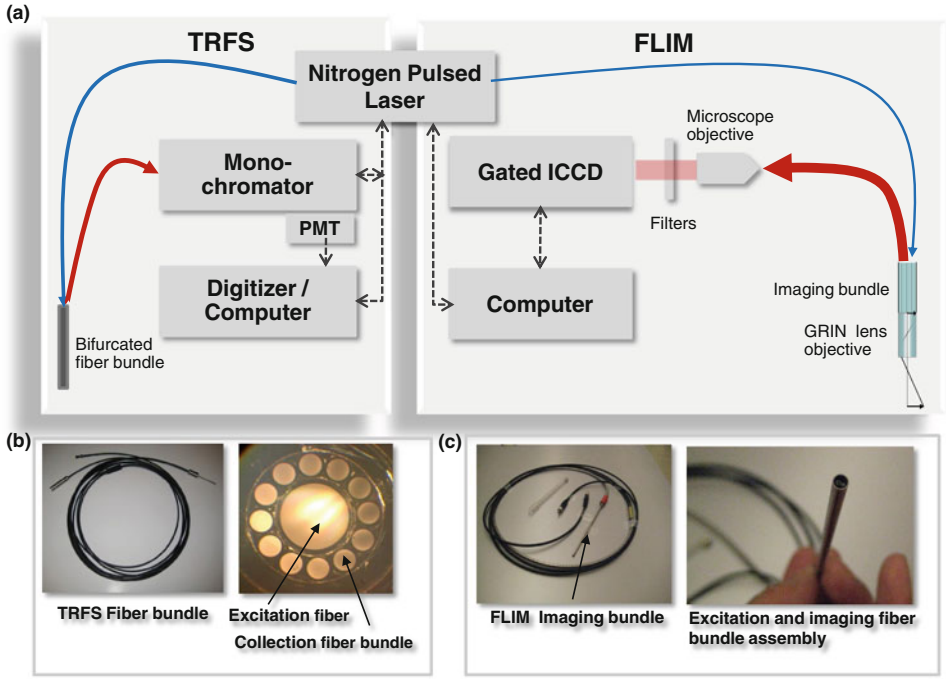

FIGURE 4. (a) Schematic of a versatile clinical system for time-resolved fluorescence studies in patients. Left panel: Setup for the TRFS mode; Right panel: Set-up for the FLIM mode. The fluorescence emission was induced *via* a 700 ps pulsed Nitrogen laser shared by the two setups. In the TRFS configuration the laser light was coupled into a multimode fiberoptic and delivered to tissue surface. Tissue fluorescence emission was collected by a ring of collection fibers, resolved by a monochromator, detected using a fast photomultiplier (PMT) tube, and resolved using a fast digitizer. In the FLIM configuration the excitation light was delivered *via* a single high numerical aperture fiberoptic and collected *via* a GRIN lens objective and a fiberoptic imaging bundle. Tissue fluorescence emission was spectrally resolved using a set of band-pass filters and detected and temporally resolved with a fast-gated ICCD camera. (b) Picture of a TRFS fiber-optic probe for collection of data from patients and picture of the distal end of this fiber probe. (c) Picture of a fiber-optic imaging bundle probe for acquisition of FLIM images from patients and picture of the distal end of this fiber bundle integrating the excitation and collection pathways. Details concerning these systems are described in Meier *et al.*[79] and Sun *et al.*[112]

5 nm interval) of fluorescence decay pulses along the entire sample fluorescence emission spectrum with a speed of ~0.8 wavelength decay profiles per second. Fluorescence decay was deconvolved using the Laguerre expansion technique. The averaged lifetime values were computed by interpolating the time the intensity decays to $1/e$ of its maximum value. Consequently, this apparatus enabled acquisition of both spectrally and temporally resolved fluorescence characteristics. Representative examples of point measurement data for normal vs. tumor are given in Figs. 5a and 5b.

For the FLIM study we used a similar apparatus and procedure as previously described by our group for clinical investigation of brain tumors in patients[112] and pre-clinical investigation of oral carcinoma in a hamster animal model.[114] The FLIM setup was based on wide-field time-domain imaging technique using a gated optical intensified CCD camera with a minimum gating time of 200 ps to resolve the fluorescence intensity decay. The fluorescence was excited and collected *via* a customized imaging probe including an excitation fiber with high numerical aperture (NA = 0.48) and a collection fiber image bundle (10,000 fibers, ~0.6 mm total diameter) and a GRIN lens objective (FOV = 4 mm). The pulsed nitrogen laser used in the TRFS system described above was also used as excitation light source in the FLIM system. The fluorescence emission was collected *via* a band-pass filter 460 ± 25 nm. Fluorescence collected within this spectral band is primarily correlated to NAD(P)H fluorescence. Both the TRFS and the FLIM system were placed on the same cart and when clinically feasible enabled collection of data from the same patient(s) with both systems. The fluorescence decays were deconvolved using the Laguerre expansion technique.[50,51] Representative examples of FLIM measurement data for normal vs. tumor are depicted in Figs. 5c and 5d. The two independent studies (TRFS[79] and FLIM,[116] respectively) demonstrated that upon 337 nm excitation features derived from the dynamics of the fluorescence decay in 460 ± 25 nm range allows for the discrimination of oral carcinoma tumors (regardless their location) from normal tissue. Overall, the tumor exhibited a faster decay dynamics when compare with

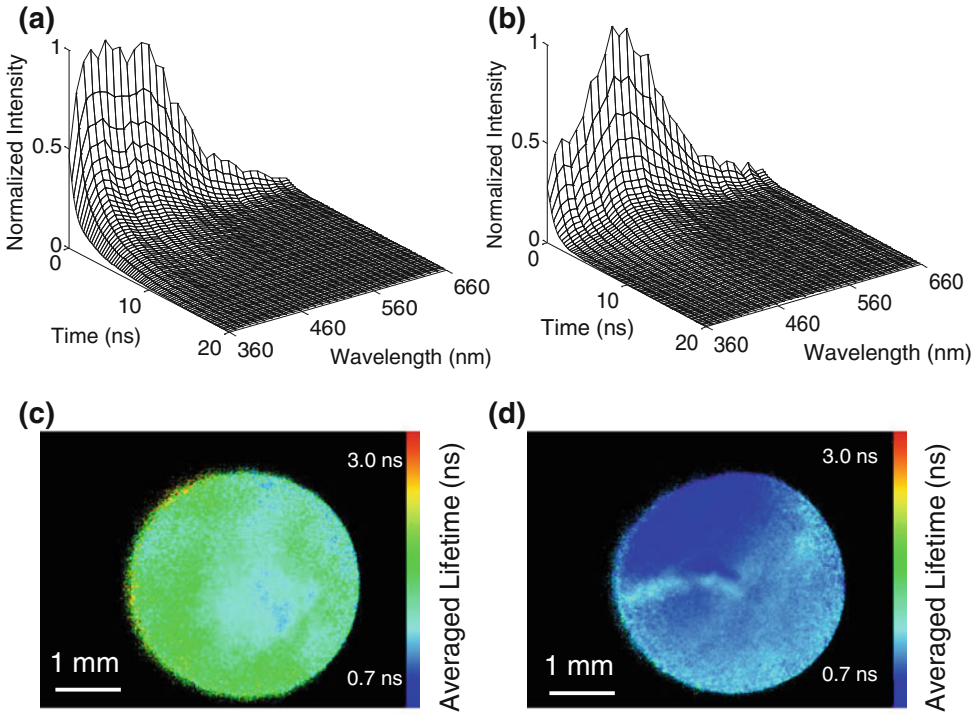

FIGURE 5. Upper panels. Representative examples of the TRFS emission of oral carcinoma located on vocal cord. (a) Normal vocal cord vs. (b) Tumor tissue. Lower panels: Representative examples of the FLIM images (4 mm field of view) of oral carcinoma located on buccal mucosa. (c) Normal mucosa vs. (d) Tumor tissue.

normal tissue. Such differences are most probably attributed to different ratios of free and bounded NAD(P)H in the two tissue types. When bound to proteins, the NAD(P)H fluorescence lifetime is known to increase multifold.[17,61] The fluorescence intensity also play an important role in distinguishing tumor vs. normal within this spectral emission range with a lower intensity in tumor tissue vs. normal tissue, trends in agreement to steady-state fluorescence intensity studies reported by other groups.[15,45,82,90,91,101,102,106,124]

Primary Brain Tumors

Intra-operative brain tumor diagnosis and delineation of surgical margins represents another important clinical target for autofluorescence technique. In contrast to other types of tumor primary brain tumors are infiltrative in nature and often do not have a well defined border. Techniques for intraoperative diagnostics are important in assisting the neurosurgeons in delineating tumor cells infiltration in normal brain tissue and to evaluate the presence of positive margins. A few groups[19,65,66,120] investigated the use of steady-state fluorescence spectroscopy (SSFS) technique complemented by diffuse reflectance spectroscopy as an intraoperative diagnostic tool. Such tool can potentially aid in either the surgical resection of gliomas or in the evaluation of radiation damage in brain tissue. A high sensitivity (94%) and specificity (93%) were reported for the delineation of normal vs. infiltrating tumor margins.[120] Paradoxically, in the same study lower sensitivity (80%) and specificity (89%) values were founded for delineating normal vs. tumor. Although promising for real-time analysis during the course of resection, no subsequent studies involving this technique have been reported.

Using the TRFS and FLIM techniques described above for oral carcinoma, our group also investigated the emission of primarily brain tumors.[12,13,112] The fluorescence lifetime characteristics of both high and low grade glioma were evaluated and contrasted against those obtained for normal cortex and normal white matter. Studies were conducted in patients undergoing surgery for brain tumor removal *via* customized fiber-optic probes that can be used to remotely access the brain tissues during conventional craniotomy procedure. The TRFS studies (337 nm excitation, 360–500 nm emission range) were reported in two publications for 17 patients[12] and 42 patients,[13] respectively. In contrast to most other cancer types, brain tumor autofluorescence is primarily associated with the emission of metabolic co-factors such as NAD(P)H and FAD. Typically, no structural proteins are present in glioma tumors unless the tumor undergoes radiation therapy and necrosis that may result in formation of collagen fibers. While scarcely reported,[121,140] pyridoxine and

glutamate decarboxylase can also contribute to the brain tissue autofluorescence with 370–400 nm wavelength range. Results from these TRFS studies demonstrated that upon 337 nm excitation both the relative intensity ratio between 390 ± 10 and 460 ± 10 nm emission bands as well as the dynamics of the fluorescence decay (averaged lifetime and Laguerre coefficients) within this bands play an important role in the discrimination normal brain tissues from both low and high grade gliomas. Representative results from these studies are depicted in Fig. 6.[12] Moreover, using parameters from both spectral and time domain we were able to classify low-grade gliomas with very high sensitivity and specificity (100 and 98%, respectively).[13] However, for high-grade gliomas the sensitivity was low (47%), while the specificity was high (94%). The low sensitivity was attributed to the heterogeneous nature of these tumors as well as phenotypic diversity. The FLIM study[112] conducted in three patients (13 sites) were in agreement with the TRFS results suggesting that the fluorescence decay dynamics at about 460 nm emission plays an important role in glioma discrimination. While these overall findings are promising, more systematic studies are needed in order to account for gliomas genetic sub-classification associated with prognostics. To our knowledge the fluorescence emission of the diverse brain tumor phenotype (e.g., malignant astrocytomas, mixed gliomas and oligodendroglioma) has not been fully investigated in order to be able to conclude on the ability of fluorescence signatures to analyze and distinguish gliomas.

Other Cancers

Detection of cervical dysplasia and cancer represents one of the most successful applications of SSFS technique in combination with reflectance spectroscopy. Pertinent reviews were recently published.[14,118] Several research groups[33,48,87,98] conducted research in this area and more recently commercial devices based on this approach have been developed. For example, LUMA™ Cervical Imaging System manufactured by MediSpectra, Inc. (Lexington, MA) received premarket approval from the FDA in 2006. To evaluate cervical abnormalities this system uses autofluorescence, diffuse reflectance backscatter, and video imaging. The FDA indicated its use as an adjunct tool to colposcopy for identification of high-grade disease in women referred for colposcopy. Another example is the Guided Therapeutics' LuViva Advanced Cervical Scan[132] currently seeking premarket approval for the early detection of cervical pre-cancer. This system integrates also autofluorescence and DRS to analyze cervical neoplasia. Interestingly, the optical spectroscopy has been found to have similar performance with colposcopy and suggested as an effective adjunct to colposcopy.[14,118] Although the overall specificity of optical spectroscopy is lower when compared with standard clinical tests, their relative high sensitivity appears to offset the lower sensitivity of the conventional tests. However, no TRFS or FLIM studies in patients were conducted in this area. The inherent nature of the fluorescence lifetime measurement can potentially improve the specificity of the fluorescence measurement conducted in cervix and consequently this can be a new area of application for time-resolved techniques. Another SSFS area of application has been the diagnosis of breast tumors. A few recent articles[53,139] reported the use of this technique as a tool to image-guide core needle biopsy of the breast (73 patients) and imaging of breast tumor surgical margins (28 patients). To our knowledge, no fluorescence lifetime study was conducted in patients diagnosed with breast tumor.

Applications of Time-Resolved Fluorescence to Human Skin

Several fluorescence techniques have been employed for the characterization of skin autofluorescence in order to evaluate their ability for analysis of skin

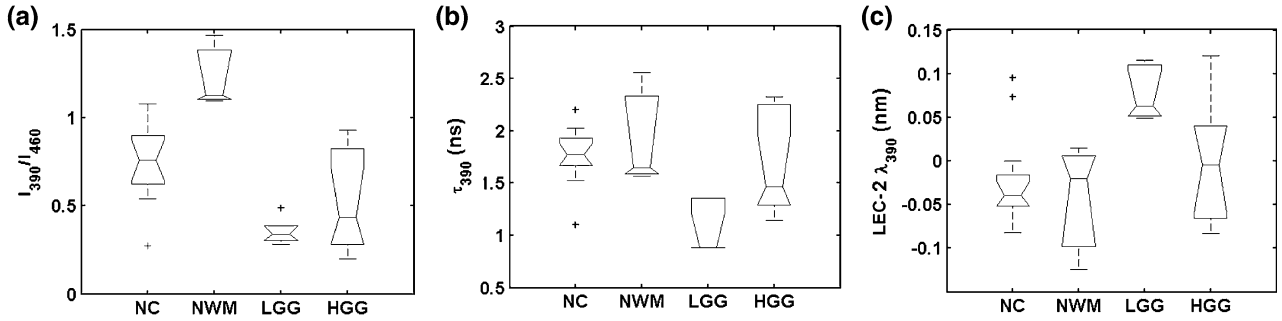

FIGURE 6. Representative examples of TRFS parameters that enable differentiation of distinct tissue types. (a) Intensity ratio 390 vs. 460; (b) average lifetime at 390 nm; (c) Laguerre coefficients at 390 nm. (NC = Normal Cortex; NWM = Normal white Matter; HGG = High Grade Glioma; LGG = Low Grade Glioma). On each box, the central mark is the median, the edges of the box are the 25th and 75th percentiles. Note: Low grade glioma demonstrates low variance as compared with high grade glioma and can be easily distinguish from normal brain tissue. Adapted from Butte *et al.*[12]

physiology, optical biopsy of skin, and detection of dermatological disorders including fungal infections, skin age, hair pigment, and cancer. Typically, the fluorescence emission of endogenous bio-molecules such as flavins, NAD(P)H coenzymes, metal-free porphyrins, components of lipofuscin, melanin, elastin, collagen and keratin is exploited as a contrast mechanism for skin characterization. The direct accessibility of skin has enabled the use of a broad range of fluorescence-based devices including multi-photon excitation and high-resolution scanning system as well as delivery and collection of light *via* rigid and free-optics. This alleviated the need for remote access of tissue *via* flexible fiber-optics that typically results in lower fluorescence light excitation and collection efficiency, and allows for an easier implementation of tissue scanning systems. Devices based on both steady-state fluorescence[11,26,44,55–57,59,73,89,96] and time-resolved fluorescence techniques were reported.[10,25,58,74,94,100] Several studies demonstrated that SSFS techniques show potential for discrimination of non-melanoma skin cancer.[10,94] However, the accuracy of discrimination depends strongly on the skin type of the patient[89] and the specificity remains low even when DRS is used to correct the fluorescence spectra.[96]

Notably, multi-photon fluorescence excitation scanning techniques including FLIM have been suggested as most appropriate for skin analysis as such approaches offer the opportunity for non-invasive optical sectioning (high spatial resolution and penetration depth) of skin and disease stage *in vivo*. Comprehensive reviews of fluorescence lifetime studies of human skin were recently reported by Koning *et al.*[59] and Roberts *et al.*[100] Over a decade ago Masters *et al.*[74] demonstrated the first use of a multi-photon scanning FLIM system to image *in vivo* human skin. Subsequently, several other groups reported the use of FLIM techniques for human skin analysis post-excision as summarized by Roberts *et al.*[100] While these *ex vivo* studies provided numerous insights in the ability of fluorescence lifetime techniques to characterize distinct features in skin related to either pathologic or non-pathologic conditions, measurements of excised skin being stored or frozen are not fully suitable for establishing the diagnosis accuracy of this technique. For example, freezing is known to lead to loss of NAD(P)H, the dominant fluorophore in the viable epidermis, thus likely to affect the fluorescence emission features of skin measured *ex vivo*. The development of a commercial clinical multiphoton tomography system, DermaInspect (JenLab GmbH), enabled a series of skin studies *in vivo* in humans.[134] This system includes a FLIM module consisting of a tunable NIR light source (titanium:sapphire laser: repetition rate of 80/90 MHz, pulse width 75–120 fs FWHM), a x-y galvano-scanner module, and a TCSPS unit. This technique is not only compatible with fast scanning but also capable of recording FLIM images in several wavelength channels simultaneously. Typically, 128 time channels covering 50 ps per channel were used for FLIM imaging. A multi-exponential fit was typically used for the analysis of fluorescence decay. A variety of dermatologic disorders (e.g., skin allergies, psoriasis, trichophytosis, and cancer) have been imaged with this system. Studies were conducted in more than 200 patients (Caucasian skin). For example, Dimitrow *et al.*[26] report a clinical study in 83 melanocytic skin lesions. Six distinctive features of malignant melanoma were specified and statistically evaluated in this study. Their results demonstrated distinct morphological differences in melanoma compared with melanocytic nevi and relatively high sensitivity values up to 95% (range: 71–95%) and specificity values up to 97% (range: 69–97%) were reported for diagnostic classification. The architectural disarray of the epidermis, poorly defined keratinocyte cell borders as well as the presence of pleomorphic or dendritic cells were found to play an important role for discrimination of distinctive features of melanoma and to improve the classification accuracy. An earlier report from the same group[25] also showed that the fluorescence emission peak at about 560 nm may enable the discrimination of melanomas from naevae.

A few TRFS systems were also tested in humans and reported,[74,94] however such reports are sparse. For example, Blackwell *et al.*[74] demonstrated the use of a TCSPC based technique to study the characteristics of time-resolved autofluorescence of skin as a function of location, gender, skin complexion and age. The system employed a pulse LED (375 nm excitation, 700 ps FWHM) as excitation source and a photomultiplier coupled to a monochromator. The time decay emission was recorded at four different emission wavelengths (442, 460, 478 and 496 nm). Data was fitted using a multi-exponential model. This study suggested that specific decay components can be related to free and bound NADH while others are related advanced glycation end product (AGE) crosslinks. However, to our knowledge subsequent efforts to extend the TRFS studies in this area have not been made.

Applications of Time-Resolved Fluorescence to Eye Diseases

A distinctive application of FLIM concerns the measurements of human eye for detection of metabolic alterations in early stages of diseases such as age-related macular degeneration and diabetic retinopathy, when no changes are visible at the eye ground. Studies in this area were primarily reported by Schweitzer

research group.[42,107–109] Time-resolved fluorescence measurements of the eye are in particular challenging due several reasons. This includes limitation concerning the use of laser light for exciting the eye fluorescence (wavelengths and permissible exposure according to the ANSI Standard limits), the efficiency of light transmission through the ocular media, and the ability to define a single image plane as the eye anatomy and its multilayer structure (cornea, lens, fundus with layers of nerve fibers and ganglion cells, *etc*.) varies with individuals. Also, the eye is an object that moves randomly. Thus, in contrast to measurements at the microscopic scale of a stationary sample, the eye movements must be compensated by online image registration. Schweitzer *et al.*[109] reported a FLIM-based laser scanner ophthalmoscope able to address such challenges. Figure 7 depicts a schematic of a clinical ophthalmoscope developed by this group and an example of data collection and online display of this instrument. The fluorescence is excited by picosecond laser (448 nm excitation, 70 ps FWHM, 80 MHz) in a 30° eye fundus field. The mean power of excitation laser light used for excitation was about 100 μW in the cornea plane. The fluorescence was detected in two spectral ranges (490–560 and 560–700 nm) by TCSPC module. The time resolution of the system was 12.2 ps. The fluorescence decays were optimally fitted by a 3-exponential model. In the fitting process the decay model was convolved with the experimentally determined instrument response function. Current studies have demonstrated that a good correspondence can be found between the first component (most frequent lifetime about 60–90 ps, amplitude about 85%) and the retinal pigment epithelium in the short wavelength channel. The second component (lifetime about 450 ps, amplitude about 12%) was found to correspond to the neuronal retina. The third component (lifetime about 3 ns, amplitude about 3%) originated from connective tissue in the choroid and was covered by the fluorescence of the crystalline lens. The local alterations can be demonstrated in images of fluorescence lifetimes, amplitudes, or relative contribution as depicted in Fig. 7. The global changes can be estimated from statistical comparison of histograms of FLIM parameters. Missing or additional appearing fluorophores can be calculated from the difference of lifetime histograms in regions of interest of patients and healthy subjects. However, the interpretation of FLIM results was found not trivial. The contribution of multiple fluorophores situated in different layers of the fundus of the eye to the overall fluorescence intensity decay cannot be fully described *via* the multiexponential model used in the study. Nevertheless, these studies demonstrate a very unique and challenging application of FLIM.

Applications of Time-Resolved Fluorescence for Research and Diagnosis of Atherosclerotic Cardiovascular Diseases

The composition of atherosclerotic plaque plays an important role on plaque instability and rupture.[47,64,67,80,86] Such event typically results in either heart attack or stroke depending on the plaque location.[64,86] Given the ability of fluorescence techniques to detect elastin, collagen, lipid components and other sources of autofluorescence in normal and diseased arterial wall these techniques were extensively explored as a means of research and diagnosis of atherosclerotic cardiovascular diseases. Importantly, most recent studies have shown the application of fluorescence techniques to the identification of plaque disruption,[18] detection of plaques with thin fibrous cap,[3] and discrimination of lipid-rich lesions.[69] Such features are a hallmark of plaque vulnerability. Both steady-state methods and time-resolved methods to characterize the biochemical composition of atherosclerotic plaques were reported.[2,3,18,29,47,67–69,80,93,104] A review of fluorescence lifetime techniques to atherosclerotic plaques was recently published by Marcu.[68]

Despite TRFS and FLIM potential for analysis of atherosclerotic diseases, most studies based on these techniques were conducted primarily *ex vivo* in excised samples or *in vivo* in atherosclerotic animal models.[2,3,6,7,18,47,69,70,80,81] Only a few recent publications present applications of a point spectroscopy TRFS device[72] and a multimodal (reflectance, fluorescence, and Raman) optical spectroscopy technique[104] for characterization of plaque fluorescence *in vivo* in patients. Both studies took advantage of the carotid endarterectomy (CEA) procedure. Carotid plaque represents an excellent study model for the validation of optical devices for detection of plaque composition in patients. The conventional clinical procedure allows for direct access of plaque *in vivo* during surgery using fiber-optic probes (with or without distal rigidity) and without the need of intravascular procedures. Also, the routine removal of the plaque during CEAs permits extensive optical studies *ex vivo* in fresh plaque specimens that account for the plaque composition heterogeneity and facilitates a direct validation of optical results against histopathological analysis. However, even in such CEA studies the total number of patients enrolled was limited. This is due to either the time available to conduct optical measurements without affecting the course of surgical procedures or the ability to mark and subsequently conduct histopathologic analysis of the exact area that underwent optical investigation. For example, our group employed a pulse-sampling based technique TRFS apparatus,[30] similar with that described above for analysis of oral and brain tumors, to study the

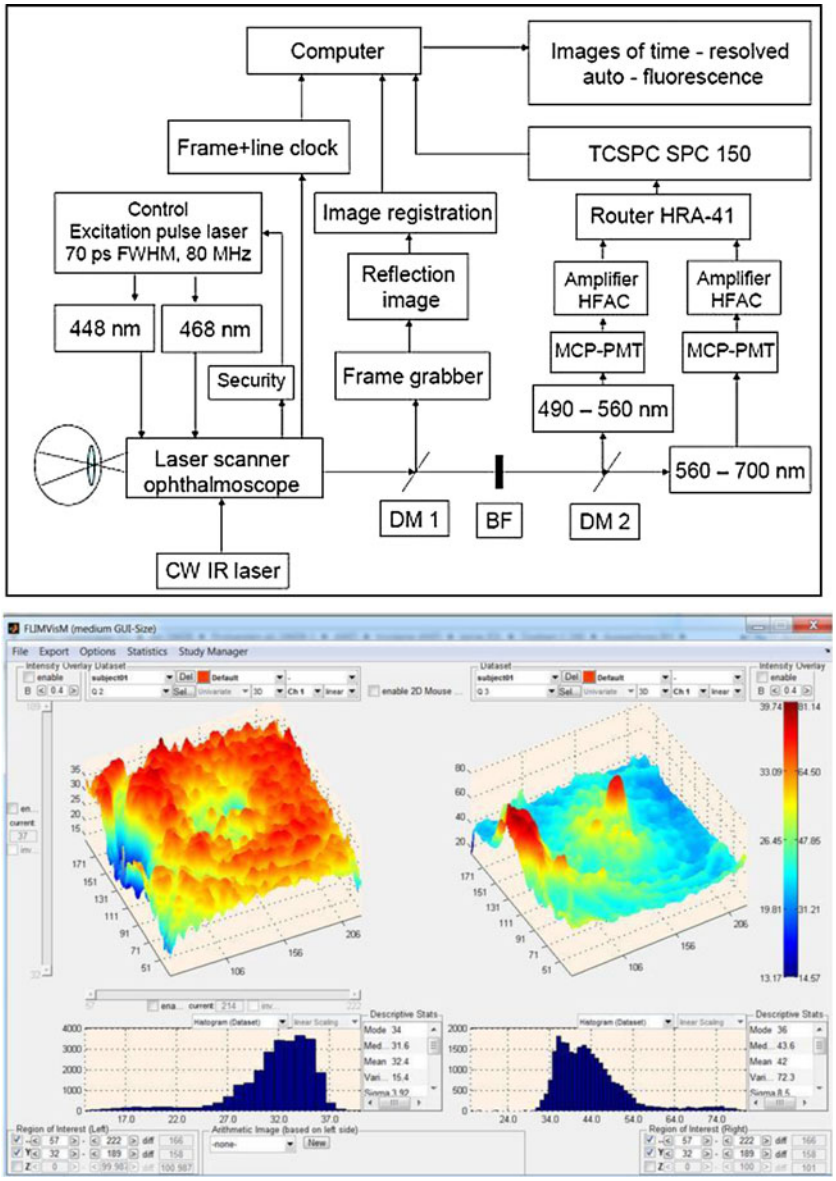

FIGURE 7. Upper panel: Schematic diagram of the scanning FLIM ophthalmoscope. The fundus is excited by ps-pulse lasers at 448 or 468 nm. The fluorescence is detected in 2 spectral intervals ch 1: 490–560 nm and ch 2: 560–700 nm using TCSPC. In addition to the excitation laser, the fundus is illuminated by a cw IR laser for online image registration. Abbreviations: Multichannel plate photomultiplier (MCP-PMT); dichroic mirror (DM); band-pass filter (BF). Lower panel: Example of FLIM data collection (screenshot) in the short wavelengths channel. In this particular case the images indicate the relative contribution of neuronal retina fluorescence (Q2—left image) and connective tissue fluorescence (Q3—right image) of a patient suffering from advanced age-related macular degeneration. The relative contribution (Q2) in the neuronal retina is expected to be reduced in the damaged macula, while the relative contribution of the connective tissue (Q3) is considerably increased in the damaged macula. The field corresponds to 150 × 150 pixels (40 × 40 μm^2 pixel size). The histograms in the bottom line are used for statistical evaluation. Courtesy of D. Schweitzer, University of Jena, Germany.

fluorescence emission of carotid plaques and to determine the ability of this technique to delineate markers of plaque vulnerability.[72] This study was conducted in a total of 65 patients (813 locations) scheduled for CEA, but clinical conditions allowed for only 14 patients (28 locations) to be investigated during the CEA intervention. Moreover, out of the 28 point measurements *in vivo* only ten of them could be correlated with the histopathologic analysis of plaque. This small final number underscores the challenge validating the fluorescence results against gold standard methods in histopathology.

While such intraoperative investigations provided insights into the ability of fluorescence measurement to analyze plaque composition *in vivo* and to analyze difference between *in vivo* and *ex vivo* measurements, this approach for data collection is impractical in actual clinical situations. Practical application would require development of flexible catheters suitable for

interrogation of the vessel wall during catheterization procedures. To our knowledge no such study has been conducted intravascularly. This is primarily due to intrinsic challenges posed by optical measurements in the presence of blood flow and in small and tortuosity of the arteries that would require advanced engineering of specialized catheters and blood flushing systems. A constraining factor is also the limited ability of most TRFS and FLIM systems to rapidly record time-resolved fluorescence data. Validation of these systems in patients would require recording of data from numerous points or from relatively large areas in order to account for atherosclerotic plaque heterogeneity and therefore to assess their diagnostic abilities. Most recent efforts attempt to address such challenges through the development of a scanning TRFS device[111,115] that can record fluorescence decays in multiple spectral bands in a few microseconds. This device was already tested *in vivo* in a pig artery[115] under intravascular ultrasound (IVUS) guidance (Fig. 8). A site viewing fiber optic and a low flow blood flushing system enabled continuous recording of fluorescence data from the arterial wall. This work demonstrated for the first time the ability of a TRFS system to collect robust in a blood vessel *in vivo* under continuous pull-back motion. Current efforts are directed towards adapting such TRFS system for recording data during radial scanning as well as pull-back motion in a similar manner as the IVUS technology. Such approach will allow a direct integration of fluorescence lifetime techniques with conventional intravascular procedure.

CHALLENGES IN CLINICAL TRANSLATION FOR TIME-RESOLVED FLUORESCENCE TECHNIQUES

Most peer-reviewed articles reporting applications of label-free fluorescence techniques for clinical diagnosis of tissues are summarized in Table 1. Close inspection of these reports clearly demonstrates that, overall, steady-state measurements (both point spectroscopy and imaging) provide a very good sensitivity but low specificity for identifying specific conditions in tissue. Complementary techniques such as diffuse reflectance spectroscopy enabled improvement of fluorescence measurement specificity. For example,

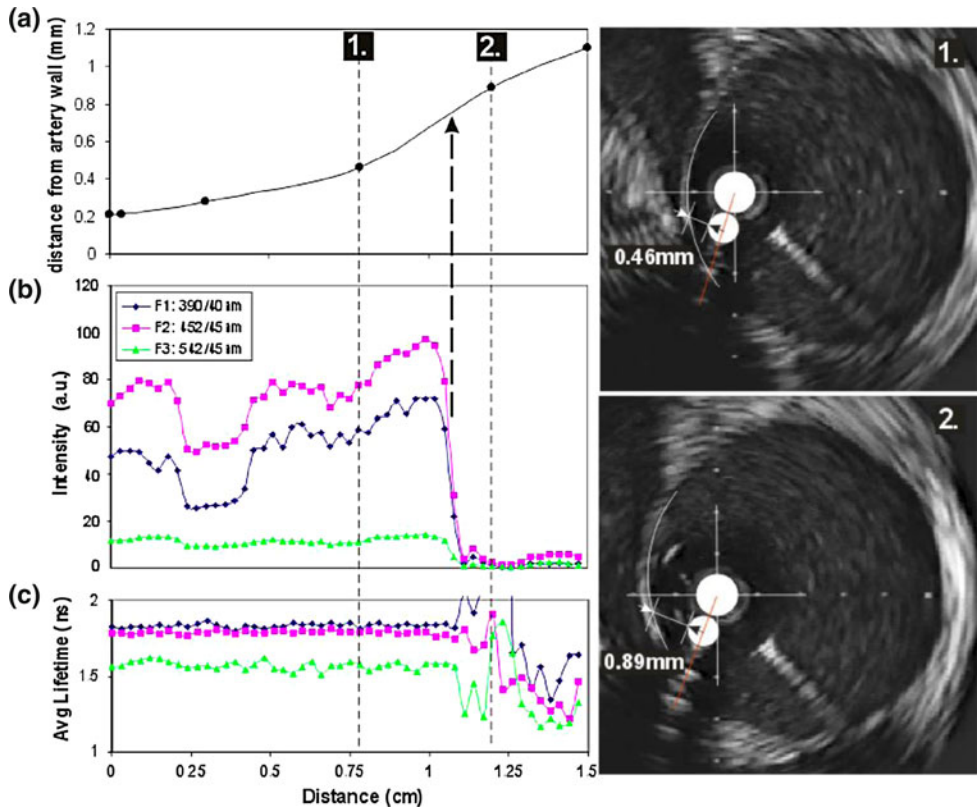

FIGURE 8. The fluorescence spectral parameters from scanning TRFS during a pull-back sequence in the right common iliac of a swine. The distance between the artery wall and catheter over the pull-back is shown at the top left in (a). The fluorescence intensity and lifetime for the three spectral bands are shown in (b) and (c) respectively. The IVUS image frames at the right show the estimated distance of the fiber optic from the arterial wall at two moments in the catheter pullback procedure. Note that while the fluorescence intensity (b) varies significantly over the scanning period, the lifetime values (c) remain relatively constant.

commercial devices based on SSFS and DRS employed in clinical trials have demonstrated that a combination of these optical signatures is very sensitive to malignant transformations, in particular detection of malignant transformations of the GI tract, bronchi, and cervix. However, even in a multimodal configuration, the overall specificity remains relatively low when compared with conventional histopathological methods.

Inherently the time-resolved measurement of fluorescence can improve the specificity of fluorescence measurements. Consequently, time-resolved techniques can play an important role in improving the overall diagnostic accuracy in tissue. Given the limited number of studies employing time-resolved techniques as well as the limited number of patients enrolled in these studies however, the diagnostic potential of this technique cannot be fully evaluated. In fact, the total number of reports involving time-resolved measurements of fluorescence for all investigated sites (e.g., GI tract, respiratory tract, oral cavity, brain, skin, eye, and arteries) is less than 25. Moreover, except for the applications of FLIM techniques to skin disease diagnosis (primarily using the commercial system DermaInspect), all studies targeting other anatomical sites have enrolled a small number of patients; typically less than 20 patients. This small number of both clinical research studies and patients enrolled clearly demonstrate that the potential of fluorescence lifetime technique for clinical diagnostics is far from being fully explored.

In general, the critical aspects that have hampered a more complete evaluation of time-resolved fluorescence techniques in patients include: (1) the rather complex and expensive instrumentation and limited availability of light sources and sensitive detectors required by time-resolved fluorescence techniques when compared with intensity/spectral techniques. This in turn limits the development of practical clinical research instrumentation; (2) the slow data acquisition speed that characterizes the majority of TRFS and FLIM devices. This limits the number of data points or images recorded from patients, thus impeding the statistic evaluation of the results; and (3) the lack of analytical methods for accurate representation of fluorescence decay profile from measurements in tissues and difficulties in the interpretation of this profile in relationship to tissue pathophysiology.

Availability and Affordability of Instrumentation for Practical Time-Resolved Measurements

The majority of the clinical studies involving TRFS or FLIM techniques described above, except for FLIM applications to skin analysis, have employed pulsed nitrogen lasers as the light source for fluorescence excitation. While these UV lasers have been reliable for most studies, their low repetition rate (<50 Hz) has precluded the development of high-speed data/image acquisition systems. Ultraviolet and blue range emission picosecond (as short as 50 ps) pulsed diode lasers (e.g., PicoQuant[135]), operating at high repetition rate (up to 40 MHz) represent a good alternative. However, the peak power output of these lasers is low in the UV range where most biological fluorophores are efficiently exited. This also results in long data acquisition times due to the need for averaging in order to improve the fluorescence signal-to-noise ratio. New picosecond pulsed solid-state lasers including compact fiber lasers are currently commercially available and could play an important role in future applications.

Mode-locked tunable Ti:Sapphire lasers have been the workhorse for multiphoton FLIM,[58] but their very high pulse repetition rate (typically at about 80–90 MHz) is not suitable for many biological fluorophores. While the repetition rates of these lasers can be reduced using appropriate pulse pickers, the fs-pulsed tunable laser systems for 2p-excitation are expensive, sometimes technically complex, and cumbersome to operate in clinical settings. Moreover, in TRFS and FLIM applications the characteristics of the excitation source are often intertwined with those of the detector.

Limited availability of fast and sensitive detectors represents another challenge for clinical applications of these techniques. Very few detectors have been used in clinical studies. These include fast MCP-PMTs or avalanche photodiodes, streak cameras (640 spectral $\times$ 480 temporal channels), gated ICCD cameras (repetition rate maximum of 10 MHz, time gate 200 ps), and TCSPS detection modules involving multiple detection channels/PMTs. Clinical FLIM systems, in particular, will benefit from the availability of fast gated, sensitive cameras that allow for wide-field imaging at high repetition rate.

While scanning methods can be relatively easily implemented in applications that enable direct access to tissue or organ of interest (e.g., skin or eye), this may not be trivial to implement in endoscopic applications or during surgery. A promising wide-field FLIM system based on a gated optical intensifier (GOI) coupled to a CCD camera was recently reported.[78] In this system, images of the exponentially decreasing fluorescence decay were recorded at 25 different time points at 250 ps intervals. A typical acquisition takes ~4 s. For each sample, five decays were acquired sequentially and averaged. Thus, the total acquisition time of this system for acquiring a FLIM image from tissue biopsy specimens was ~20 s.

Overall, a broader use of TRFS and FLIM techniques in clinical settings relies on the availability of affordable picosecond pulsed lasers and fast and

sensitive detector technologies. Technical solutions that enable the use of multiple wavelengths (tunable light sources) for tissue excitation as well as resolve the fluorescence decays at multiple wavelengths simultaneously (hyperspectral TRFS or FLIM detection)[23,115] can also play an important role in the evaluation of lifetime fluorescence techniques potential for clinical diagnosis of diseases.

Analysis of Fluorescence Decay and Interpretation of the Decay Profile

Another challenge is posed by the complexity of fluorescence decay profiles derived from tissue measurements and our ability to accurately represent and interpret the rich information content within this decay profile. Not only is the tissue autofluorescence generated by several biological molecules with overlapping spectral emission, but also the fluorescence emission characteristics of these biological molecules depends on their physiochemical environment. In addition, the effects of tissue architecture may affect the volumetric/depth distribution of the fluorophores. Consequently, for tissue autofluorescence, there is no a priori knowledge of the intensity decay model.

The majority of fluorescence lifetime studies conducted in patients used an exponential approximation (typically bi-exponential) to evaluate the fluorescence decay dynamics. While this approach may provide some insight into the type and number of the dominant fluorescent molecules in tissue, this representation most likely cannot capture the number of actual multi-exponential components in the decay profile. Ultimately, the bi-exponential approximation of complex biological tissue fluorescence is just a convenient way to analyze and display the TRFS and FLIM data, but this representation may not capture or use the entire information content within the intensity decay profile.

The use of Laguerre functions as a means of representing the fluorescence decay characteristics has some intrinsic advantages as described above. This deconvolution technique has primarily been used by our research group. We demonstrated that this method provides a model-free representation of decay dynamics as well as a much faster approach to fIRF deconvolution. Subsequently it supports the further development of real-time (on-line) TRFS or FLIM diagnostic systems.

The ability to accurately retrieve and parameterize the intensity decay profile is only a step towards resolving the fluorescence decay from biological tissues. A subsequent challenge emerges from the limited ability to interpret the numerous fluorescence parameters as a function of tissue patho-physiological conditions. Validation of fluorescence data acquired *in vivo* is based on conventional histopathological analysis conducted on tissue specimens/biopsy removed from optically interrogated tissue regions. This is subject to both sampling error as well as changes in tissue conditions post-excision (physiology, metabolism, morphology, *etc.*). Consequently a quantitative interpretation of the fluorescence decay data is virtually impossible, in particular for metabolically active tissues such as tumors. New paradigms for analysis fluorescence decay and interpretation of time-resolved decay parameters as a function of tissue pathophysiology are needed in order to evaluate the full diagnostic potential of time-resolved techniques.

In addition, problems with the interpretation of decay profiles may arise when comparing information generated with different instruments. The instrument response function as well as the computational method for fluorescence decay profile analysis is likely to affect the numerical values of various parameters used for characterization of fluorescence decay (e.g., lifetime(s), decay constants, Laguerre coefficients, *etc.*). A "universal standard" for calibration of different time-resolved fluorescence instrumentation could play an important role in analytical chemistry/biochemistry and biophysics, but such standards may still be challenged when the instrumentation is used in tissues analysis.

Given the biological complexity of tissues and subsequently the complexity of the fluorescence decays measured from biological tissue, in our view the development of a clinical instrument would rather benefit from calibration procedures that enable systematic identification of certain conditions in tissue, rather than accurate recovery of specific decay parameters. While absolute decay parameter values can be used for a quantitative interpretation of fluorescence data and are essential for research in biochemistry and biophysics, this may not necessarily fully address the needs for clinical tissue diagnosis. Perhaps, a method for robust qualitative analysis of fluorescence data capable of providing a fast and accurate recognition/staging of specific pathologies in tissues would better serve the immediate clinical needs.

Limited Tissue Penetration Depth

An inherent challenge for the fluorescence techniques is the shallow penetration depth of the excitation light. Single-photon excitation (ultraviolet range) provides a tissue interrogation depth below 0.5 mm, while multi-photon excitation (near-infrared range) enables higher penetration but still below 1.5–2 mm. Consequently, this confines the applicability of TRFS and FLIM to tissue/organ surfaces. However, these techniques are very sensitive to early pathological

molecular changes that typically occur at the tissue/organ surface and are even capable of spatially resolving such changes with high resolution (e.g., multi-photon based systems). Generally, conventional imaging or spectroscopic techniques with higher penetration depth cannot sense and resolve early pathological transformations. Also, most conventional imaging techniques (e.g., optical coherence tomography) provide structural rather than biochemical and functional information. Perhaps, future development of hybrid systems combining techniques capable of providing complementary information and of interrogating tissues at variable depths with "pathologic" resolution will expand the diagnostic ability of current fluorescence-based techniques.

CONCLUSION

Clinically compatible time-resolved fluorescence spectroscopy and imaging systems developed by several research groups have demonstrated that fluorescence lifetime provides a means of achieving optical molecular contrast in diseased tissues measured in patients. Also, they have shown that fluorescence lifetime contrast can be used in tissue characterization and diagnosis. However, as reported in literature, the total number of studies as well as patients involved in TRFS or FLIM clinical research is very small. Thus, no definitive conclusion can be drawn regarding the potential of these techniques for medical diagnosis. Systematic studies of the fluorescence decay characteristics in patients along with evaluation of intra-patient data variability are critical for a complete assessment of fluorescence lifetime techniques ability for accurate clinical diagnosis.

Current efforts toward identifying new technical solutions for fast recording of spectrally resolved fluorescence lifetime information, combined with advancement of new analytical methods for fast processing of the fluorescence intensity decay data, are enablers for further development of compact diagnostic TRFS and FLIM systems. Such solutions can initially facilitate further development of practical devices for clinical research studies and methodical evaluation of their diagnostic potential. Extrapolating on the current clinical successes of the fluorescence systems based on intensity and spectral information only, it is anticipated that the addition of time-resolved information will improve the accuracy for diagnostics of these devices.

Since several SSFS devices, including commercial systems, have been extensively evaluated in patients and involved in FDA approved clinical trials, a potential approach to rapid evaluation of TRFS and FLIM devices in the clinical environment is adding a simple time-resolved detection module to existing SSFS instrumentation platforms. This can provide a direct venue to systematically verify whether and how lifetime information can be used to improve the specificity of fluorescence measurements. A successful outcome will alleviate the need for coupling SSFS devices with other spectroscopic techniques (e.g., diffuse reflectance spectroscopy) or other cumbersome intensity calibration and correction procedures. Advancement of simple solutions for clinical implementation of TRFS and FLIM devices has the potential to impact the clinical management of disease by enabling early diagnosis, real-time detection of surgical margins, and monitoring the effect of therapeutic interventions.

ACKNOWLEDGMENTS

The author would like to thank Dr. D. Schweitzer (University of Jena, Germany) and Dr. G. Wagnieres (Swiss Federal Institute of Technology) for providing support material for this review and their insightful comments. We also thank Dr. H. Xie for his help with literature review. Work in the author's laboratory has been supported by the National Institutes of Health (R01 HL67377, R21 RR 025818).

REFERENCES

[1]Andersson-Engels, S., C. Klinteberg, K. Svanberg, and S. Svanberg. In vivo fluorescence imaging for tissue diagnostics. *Phys. Med. Biol.* 42:815–824, 1997.

[2]Angheloiu, G. O., J. T. Arendt, M. G. Muller, A. S. Haka, I. Georgakoudi, J. T. Motz, O. R. Scepanovic, B. D. Kuban, J. Myles, F. Miller, E. A. Podrez, M. Fitzmaurice, J. R. Kramer, and M. S. Feld. Intrinsic fluorescence and diffuse reflectance spectroscopy identify superficial foam cells in coronary plaques prone to erosion. *Arterioscler. Thromb. Vasc. Biol.* 26:1594–1600, 2006.

[3]Arakawa, K., K. Isoda, T. Ito, K. Nakajima, T. Shibuya, and F. Ohsuzu. Fluorescence analysis of biochemical constituents identifies atherosclerotic plaque with a thin fibrous cap. *Arterioscler. Thromb. Vasc. Biol.* 22:1002–1007, 2002.

[4]Arens, C., D. Reussner, H. Neubacher, J. Woenckhaus, and H. Glanz. Spectrometric measurement in laryngeal cancer. *Eur. Arch. Otorhinolaryngol.* 263:1001–1007, 2006.

[5]Ashjian, P., A. Elbarbary, P. Zuk, D. A. DeUgarte, P. Benhaim, L. Marcu, and M. H. Hedrick. Noninvasive in situ evaluation of osteogenic differentiation by time-resolved laser-induced fluorescence spectroscopy. *Tissue Eng.* 10:411–420, 2004.

[6]Baraga, J. J., R. P. Rava, P. Taroni, C. Kittrell, M. Fitzmaurice, and M. S. Feld. Laser induced fluorescence spectroscopy of normal and atherosclerotic human aorta

using 306–310 nm excitation. *Lasers Surg. Med.* 10:245–261, 1990.

[7]Bartorelli, A. L., M. B. Leon, Y. Almagor, L. G. Prevosti, J. A. Swain, C. L. McIntosh, R. F. Neville, M. D. House, and R. F. Bonner. In vivo human atherosclerotic plaque recognition by laser-excited fluorescence spectroscopy. *J. Am. Coll. Cardiol.* 17:160B–168B, 1991.

[8]Berezin, M. Y., and S. Achilefu. Fluorescence lifetime measurements and biological imaging. *Chem. Rev.* 110:2641–2684, 2010.

[9]Bigio, I. J., and J. R. Mourant. Ultraviolet and visible spectroscopies for tissue diagnostics: fluorescence spectroscopy and elastic-scattering spectroscopy. *Phys. Med. Biol.* 42:803–814, 1997.

[10]Blackwell, J., K. M. Katika, L. Pilon, K. M. Dipple, S. R. Levin, and A. Nouvong. In vivo time-resolved autofluorescence measurements to test for glycation of human skin. *J. Biomed. Opt.* 13:014004, 2008.

[11]Brancaleon, L., A. J. Durkin, J. H. Tu, G. Menaker, J. D. Fallon, and N. Kollias. In vivo fluorescence spectroscopy of nonmelanoma skin cancer. *Photochem. Photobiol.* 73:178–183, 2001. .

[12]Butte, P. V., Q. Fang, J. A. Jo, W. H. Yong, B. K. Pikul, K. L. Black, and L. Marcu. Intraoperative delineation of primary brain tumors using time-resolved fluorescence spectroscopy. *J. Biomed. Opt.* 15:027008, 2010.

[13]Butte, P. V., A. N. Mamelak, M. Nuno, S. I. Bannykh, K. L. Black, and L. Marcu. Fluorescence lifetime spectroscopy for guided therapy of brain tumors. *Neuroimage* 54(Suppl 1):S125–S135, 2011.

[14]Cardenas-Turanzas, M., J. A. Freeberg, J. L. Benedet, E. N. Atkinson, D. D. Cox, R. Richards-Kortum, C. MacAulay, M. Follen, and S. B. Cantor. The clinical effectiveness of optical spectroscopy for the in vivo diagnosis of cervical intraepithelial neoplasia: where are we? *Gynecol. Oncol.* 107:S138–S146, 2007.

[15]Chaturvedi, P., S. K. Majumder, H. Krishna, S. Muttagi, and P. K. Gupta. Fluorescence spectroscopy for noninvasive early diagnosis of oral mucosal malignant and potentially malignant lesions. *J. Cancer Res. Ther.* 6:497–502, 2010.

[16]Chen, H. M., C. P. Chiang, C. You, T. C. Hsiao, and C. Y. Wang. Time-resolved autofluorescence spectroscopy for classifying normal and premalignant oral tissues. *Lasers Surg. Med.* 37:37–45, 2005.

[17]Chorvat, D., and A. Chorvatova. Multi-wavelength fluorescence lifetime spectroscopy: a new approach to the study of endogenous fluorescence in living cells and tissues. *Lasers Phys. Lett.* 6:175–193, 2009.

[18]Christov, A., E. Dai, M. Drangova, L. Liu, G. S. Abela, P. Nash, G. McFadden, and A. Lucas. Optical detection of triggered atherosclerotic plaque disruption by fluorescence emission analysis. *Photochem. Photobiol.* 72:242–252, 2000.

[19]Croce, A. C., S. Fiorani, D. Locatelli, R. Nano, M. Ceroni, F. Tancioni, E. Giombelli, E. Benericetti, and G. Bottiroli. Diagnostic potential of autofluorescence for an assisted intraoperative delineation of glioblastoma resection margins. *Photochem. Photobiol.* 77:309–318, 2003.

[20]Cubeddu, R., D. Comelli, C. D'Andrea, P. Taroni, and G. Valentini. Time-resolved fluorescence imaging in biology and medicine. *J. Phys. D: Appl. Phys* 35:R61–R76, 2002.

[21]Curvers, W. L., R. Singh, L. M. Song, H. C. Wolfsen, K. Ragunath, K. Wang, M. B. Wallace, P. Fockens, and J. J. Bergman. Endoscopic tri-modal imaging for detection of early neoplasia in Barrett's oesophagus: a multi-centre feasibility study using high-resolution endoscopy, autofluorescence imaging and narrow band imaging incorporated in one endoscopy system. *Gut* 57:167–172, 2008.

[22]Das, B. B., F. Liu, and R. R. Alfano. Time-resolved fluorescence and photon migration studies in biomedical and model random media. *Rep. Prog. Phys.* 60:227–292, 1997.

[23]De Beule, P. A. A., C. Dunsby, N. P. Galletly, G. W. Stamp, A. C. Chu, U. Anand, P. Anand, C. D. Benham, A. Naylor, and P. M. W. French. A hyperspectral fluorescence lifetime probe for skin cancer diagnosis. *Rev. Sci. Instrum.* 78:123101, 2007.

[24]Delank, W., B. Khanavkar, J. A. Nakhosteen, and W. Stoll. A pilot study of autofluorescent endoscopy for the in vivo detection of laryngeal cancer. *Laryngoscope* 110:368–373, 2000.

[25]Dimitrow, E., I. Riemann, A. Ehlers, M. J. Koehler, J. Norgauer, P. Elsner, K. Konig, and M. Kaatz. Spectral fluorescence lifetime detection and selective melanin imaging by multiphoton laser tomography for melanoma diagnosis. *Exp. Dermatol.* 18:509–515, 2009.

[26]Dimitrow, E., M. Ziemer, M. J. Koehler, J. Norgauer, K. Konig, P. Elsner, and M. Kaatz. Sensitivity and specificity of multiphoton laser tomography for in vivo and ex vivo diagnosis of malignant melanoma. *J. Invest. Dermatol.* 129:1752–1758, 2009.

[27]Dognitz, N., D. Salomon, M. Zellweger, J. P. Ballini, T. Gabrecht, N. Lange, H. van den Bergh, and G. Wagnieres. Comparison of ALA- and ALA hexyl-ester-induced PpIX depth distribution in human skin carcinoma. *J. Photochem. Photobiol. B* 93:140–148, 2008.

[28]Elson, D., N. Galletly, C. Talbot, J. Requejo-Isidro, J. McGinty, C. Dunsby, P. Lanigan, I. Munro, R. Benninger, P. de Beule, E. Auksorius, L. Hegyi, A. Sandison, A. Wallace, P. Soutter, M. Neil, J. Lever, G. Stamp, and P. French. Multidimensional Fluorescence Imaging applied to biological tissues. In: Reviews in Fluorescence, edited by C. Geddes, and J. R. Lakowicz. New York: Springer, 2006, pp. 477–524.

[29]Elson, D. S., J. A. Jo, and L. Marcu. Miniaturized side-viewing imaging probe for fluorescence lifetime imaging (FLIM): validation with fluorescence dyes, tissue structural proteins and tissue specimens. *New. J. Phys.* 9:127, 2007.

[30]Fang, Q., T. Papaioannou, J. A. Jo, R. Vaitha, K. Shastry, and L. Marcu. Time-domain laser-induced fluorescence apparatus for clinical diagnostics. *Rev. Sci. Instrum.* 75:151–162, 2004.

[31]Fawzy, Y., and H. Zeng. Intrinsic fluorescence spectroscopy for endoscopic detection and localization of the endobronchial cancerous lesions. *J. Biomed. Opt.* 13:064022, 2008.

[32]Fite, B. Z., M. Decaris, Y. Sun, Y. Sun, A. Lam, C. K. Ho, J. K. Leach, and L. Marcu. Noninvasive multimodal evaluation of bioengineered cartilage constructs combining time-resolved fluorescence and ultrasound imaging. *Tissue Eng. C: Methods* 17:495–504, 2011.

[33]Freeberg, J. A., D. M. Serachitopol, N. McKinnon, R. Price, E. N. Atkinson, D. D. Cox, C. MacAulay, R. Richards-Kortum, M. Follen, and B. Pikkula. Fluorescence and reflectance device variability throughout the progression of a phase II clinical trial to detect and screen for cervical neoplasia using a fiber optic probe. *J. Biomed. Opt.* 12:034015, 2007.

[34]Gabrecht, T., T. Glanzmann, L. Freitag, B. C. Weber, H. van den Bergh, and G. Wagnieres. Optimized autofluorescence bronchoscopy using additional backscattered red light. *J. Biomed. Opt*. 12:064016, 2007.
[35]Gabrecht, T., B. Lovisa, F. Borle, and G. Wagnieres. Design of an endoscopic optical reference to be used for autofluorescence bronchoscopy with a commercially available diagnostic autofluorescence endoscopy (DAFE) system. *Phys. Med. Biol*. 52:N163–N171, 2007.
[36]Gabrecht, T., A. Radu, P. Grosjean, B. Weber, G. Reichle, L. Freitag, P. Monnier, H. van den Bergh, and G. Wagnieres. Improvement of the specificity of cancer detection by autofluorescence imaging in the tracheobronchial tree using backscattered violet light. *Photodiagn. Photodyn. Ther*. 5:2–9, 2008.
[37]Georgakoudi, I., W. L. Rice, M. Hronik-Tupaj, and D. L. Kaplan. Optical spectroscopy and imaging for the noninvasive evaluation of engineered tissues. *Tissue Eng. B Rev*. 14:321–340, 2008.
[38]Gilbert, S., J. D. Luketich, and N. A. Christie. Fluorescent bronchoscopy. *Thorac. Surg. Clin*. 14:71–77, viii, 2004.
[39]Glanzmann, T., J. P. Ballini, H. van den Bergh, and G. Wagnières. Time-resolved spectrofluorometer for clinical tissue characterization during endoscopy. *Rev. Sci. Instrum*. 70:4067–4077, 2009.
[40]Goujon, D., M. Zellweger, A. Radu, P. Grosjean, B. C. Weber, H. van den Bergh, P. Monnier, and G. Wagnieres. In vivo autofluorescence imaging of early cancers in the human tracheobronchial tree with a spectrally optimized system. *J. Biomed. Opt*. 8:17–25, 2003.
[41]Haj-Hosseini, N., J. Richter, S. Andersson-Engels, and K. Wardell. Optical touch pointer for fluorescence guided glioblastoma resection using 5-aminolevulinic acid. *Lasers Surg. Med*. 42:9–14, 2010.
[42]Hammer, M., E. Konigsdorffer, C. Liebermann, C. Framme, G. Schuch, D. Schweitzer, and J. Strobel. Ocular fundus auto-fluorescence observations at different wavelengths in patients with age-related macular degeneration and diabetic retinopathy. *Graefes. Arch. Clin. Exp. Ophthalmol*. 246:105–114, 2008.
[43]Hanibuchi, M., S. Yano, Y. Nishioka, T. Miyoshi, K. Kondo, H. Uehara, and S. Sone. Autofluorescence bronchoscopy, a novel modality for the early detection of bronchial premalignant and malignant lesions. *J. Med. Invest*. 54:261–266, 2007.
[44]Hegyi, J., V. Hegyi, T. Ruzicka, P. Arenberger, and C. Berking. New developments in fluorescence diagnostics. *J. Dtsch. Dermatol. Ges*. 9:368–372, 2011.
[45]Heintzelman, D. L., U. Utzinger, H. Fuchs, A. Zuluaga, K. Gossage, A. M. Gillenwater, R. Jacob, B. Kemp, and R. R. Richards-Kortum. Optimal excitation wavelengths for in vivo detection of oral neoplasia using fluorescence spectroscopy. *Photochem. Photobiol*. 72:103–113, 2000.
[46]Herth, F. J., A. Ernst, and H. D. Becker. Autofluorescence bronchoscopy—a comparison of two systems (LIFE and D-Light). *Respiration* 70:395–398, 2003.
[47]Honda, Y., and P. J. Fitzgerald. Frontiers in intravascular imaging technologies. *Circulation* 117:2024–2037, 2008.
[48]Huh, W. K., R. M. Cestero, F. A. Garcia, M. A. Gold, R. S. Guido, K. McIntyre-Seltman, D. M. Harper, L. Burke, S. T. Sum, R. F. Flewelling, and R. D. Alvarez. Optical detection of high-grade cervical intraepithelial neoplasia in vivo: results of a 604-patient study. *Am. J. Obstet. Gynecol*. 190:1249–1257, 2004.
[49]Huttenberger, D., T. Gabrecht, G. Wagnieres, B. Weber, A. Linder, H. J. Foth, and L. Freitag. Autofluorescence detection of tumors in the human lung–spectroscopical measurements in situ, in an in vivo model and in vitro. *Photodiagn. Photodyn. Ther*. 5:139–147, 2008.
[50]Jo, J. A., Q. Fang, T. Papaioannou, J. D. Baker, A. H. Dorafshar, T. Reil, J. H. Qiao, M. C. Fishbein, J. A. Freischlag, and L. Marcu. Laguerre-based method for analysis of time-resolved fluorescence data: application to in vivo characterization and diagnosis of atherosclerotic lesions. *J. Biomed. Opt*. 11:021004, 2006.
[51]Jo, J. A., Q. Fang, T. Papaioannou, and L. Marcu. Fast model-free deconvolution of fluorescence decay for analysis of biological systems. *J. Biomed. Opt*. 9:743–752, 2004.
[52]Kara, M.-A., F. P. Peters, P. Fockens, F. J. ten Kate, and J. J. Bergman. Endoscopic video-autofluorescence imaging followed by narrow band imaging for detecting early neoplasia in Barrett's esophagus. *Gastrointest. Endosc*. 64:176–185, 2006.
[53]Keller, M. D., S. K. Majumder, M. C. Kelley, I. M. Meszoely, F. I. Boulos, G. M. Olivares, and A. Mahadevan-Jansen. Autofluorescence and diffuse reflectance spectroscopy and spectral imaging for breast surgical margin analysis. *Lasers Surg. Med*. 42:15–23, 2010.
[54]Kobayashi, H., M. Ogawa, R. Alford, P. L. Choyke, and Y. Urano. New strategies for fluorescent probe design in medical diagnostic imaging. *Chem. Rev*. 110:2620–2640, 2010.
[55]Koehler, M. J., K. Konig, P. Elsner, R. Buckle, and M. Kaatz. In vivo assessment of human skin aging by multiphoton laser scanning tomography. *Opt. Lett*. 31:2879–2881, 2006.
[56]Koetsier, M., E. Nur, H. Chunmao, H. L. Lutgers, T. P. Links, A. J. Smit, G. Rakhorst, and R. Graaff. Skin color independent assessment of aging using skin autofluorescence. *Opt. Express* 18:14416–14429, 2010.
[57]Kollias, N., G. Zonios, and G. N. Stamatas. Fluorescence spectroscopy of skin. *Vib. Spectrosc*. 28:17–23, 2002.
[58]Konig, K. Clinical multiphoton tomography. *J. Biophotonics* 1:13–23, 2008.
[59]Konig, K., A. Ehlers, I. Riemann, S. Schenkl, R. Buckle, and M. Kaatz. Clinical two-photon microendoscopy. *Microsc. Res. Tech*. 70:398–402, 2007.
[60]Kumar, S., C. Dunsby, P. A. De Beule, D. M. Owen, U. Anand, P. M. Lanigan, R. K. Benninger, D. M. Davis, M. A. Neil, P. Anand, C. Benham, A. Naylor, and P. M. French. Multifocal multiphoton excitation and time correlated single photon counting detection for 3-D fluorescence lifetime imaging. *Opt. Express*. 15:12548–12561, 2007.
[61]Lakowicz, J. R. Principles of Fluorescence Spectroscopy (3rd ed.). New York: Kluwer/Plenum, 2006.
[62]Lam, S., C. MacAulay, J. C. leRiche, and B. Palcic. Detection and localization of early lung cancer by fluorescence bronchoscopy. *Cancer* 89:2468–2473, 2000.
[63]Lane, P. M., T. Gilhuly, P. Whitehead, H. Zeng, C. F. Poh, S. Ng, P. M. Williams, L. Zhang, M. P. Rosin, and C. E. MacAulay. Simple device for the direct visualization of oral-cavity tissue fluorescence. *J. Biomed. Opt*. 11:024006, 2006.
[64]Libby, P., and M. Aikawa. Stabilization of atherosclerotic plaques: new mechanisms and clinical targets. *Nat. Med*. 8:1257–1262, 2002.
[65]Lin, W. C., A. Mahadevan-Jansen, M. D. Johnson, R. J. Weil, and S. A. Toms. In vivo optical spectroscopy detects

radiation damage in brain tissue. *Neurosurgery* 57:518–525; discussion 518–525, 2005.
[66]Lin, W. C., S. A. Toms, M. Johnson, E. D. Jansen, and A. Mahadevan-Jansen. In vivo brain tumor demarcation using optical spectroscopy. *Photochem. Photobiol.* 73:396–402, 2001.
[67]MacNeill, B. D., H. C. Lowe, M. Takano, V. Fuster, and I. K. Jang. Intravascular modalities for detection of vulnerable plaque: current status. *Arterioscler. Thromb. Vasc. Biol.* 23:1333–1342, 2003.
[68]Marcu, L. Fluorescence lifetime in cardiovascular diagnostics. *J. Biomed. Opt.* 15:011106, 2010.
[69]Marcu, L., M. C. Fishbein, J. M. Maarek, and W. S. Grundfest. Discrimination of human coronary artery atherosclerotic lipid-rich lesions by time-resolved laser-induced fluorescence spectroscopy. *Arterioscler. Thromb. Vasc. Biol.* 21:1244–1250, 2001.
[70]Marcu, L., W. S. Grundfest, and M. C. Fishbein. Time-resolved laser-induced fluorescence spectroscopy for staging atherosclerotic lesions. In: Handbook of Biomedical Fluorescence, edited by M.-A. Mycek, and B. W. Pogue. New York: Marcel Dekker, Inc, 2003, pp. 397–429.
[71]Marcu, L., J. A. Jo, and P. Butte. Fluorescence lifetime spectroscopy in cardio and neuroimaging. In: Advances in Optical Imaging for Clinical Medicine, edited by N. Iftimia, W. R. Brugge, and D. X. Hammer. New Jersey: Wiley, 2011.
[72]Marcu, L., J. A. Jo, Q. Fang, T. Papaioannou, T. Reil, J. H. Qiao, J. D. Baker, J. A. Freischlag, and M. C. Fishbein. Detection of rupture-prone atherosclerotic plaques by time-resolved laser-induced fluorescence spectroscopy. *Atherosclerosis* 204:156–164, 2009.
[73]Masters, B., and P. So. Confocal microscopy and multiphoton excitation microscopy of human skin in vivo. *Opt. Express* 8:2–10, 2001.
[74]Masters, B. R., P. T. So, and E. Gratton. Multiphoton excitation fluorescence microscopy and spectroscopy of in vivo human skin. *Biophys. J.* 72:2405–2412, 1997.
[75]Mayinger, B., P. Horner, M. Jordan, C. Gerlach, T. Horbach, W. Hohenberger, and E. G. Hahn. Light-induced autofluorescence spectroscopy for tissue diagnosis of GI lesions. *Gastrointest. Endosc.* 52:395–400, 2000.
[76]Mayinger, B., P. Horner, M. Jordan, C. Gerlach, T. Horbach, W. Hohenberger, and E. G. Hahn. Light-induced autofluorescence spectroscopy for the endoscopic detection of esophageal cancer. *Gastrointest. Endosc.* 54:195–201, 2001.
[77]McGinty, J., N. P. Galletly, C. Dunsby, I. Munro, D. S. Elson, J. Requejo-Isidro, P. Cohen, R. Ahmad, A. Forsyth, A. V. Thillainayagam, M. A. Neil, P. M. French, and G. W. Stamp. Wide-field fluorescence lifetime imaging of cancer. *Biomed. Opt. Express* 1:627–640, 2010.
[78]McGinty, J., N. P. Galletly, C. Dunsby, I. Munro, D. S. Elson, J. Requejo-Isidro, P. Cohen, R. Ahmad, A. Forsyth, A. V. Thillainayagam, M. A. A. Neil, P. M. W. French, and G. W. Stamp. Wide-field fluorescence lifetime imaging of cancer. *Biomed. Opt. Expres.* 1:627–640, 2010.
[79]Meier, J. D., H. Xie, Y. Sun, Y. Sun, N. Hatami, B. Poirier, L. Marcu, and D. G. Farwell. Time-resolved laser-induced fluorescence spectroscopy as a diagnostic instrument in head and neck carcinoma. *Otolaryngol. Head Neck Surg.* 142:838–844, 2010.
[80]Moreno, P. R., and J. E. Muller. Identification of high-risk atherosclerotic plaques: a survey of spectroscopic methods. *Curr. Opin. Cardiol.* 17:638–647, 2002.
[81]Morguet, A. J., B. Korber, B. Abel, H. Hippler, V. Wiegand, and H. Kreuzer. Autofluorescence spectroscopy using a XeCl excimer laser system for simultaneous plaque ablation and fluorescence excitation. *Lasers Surg. Med.* 14:238–248, 1994.
[82]Muller, M. G., T. A. Valdez, I. Georgakoudi, V. Backman, C. Fuentes, S. Kabani, N. Laver, Z. Wang, C. W. Boone, R. R. Dasari, S. M. Shapshay, and M. S. Feld. Spectroscopic detection and evaluation of morphologic and biochemical changes in early human oral carcinoma. *Cancer* 97:1681–1692, 2003.
[83]Mycek, M.-A., K. Vishwanath, K. T. Schomacker, and N. S. Nishioka. Fluorescence spectroscopy for in vivo discrimination of pre-malignant colonic lesions. *OSA/BOSD*, 2000.
[84]Mycek, M.-A., and B. W. Pogue. Handbook of Biomedical Fluorescence. New York: Marcel Dekker, Inc., 2003.
[85]Mycek, M. A., K. T. Schomacker, and N. S. Nishioka. Colonic polyp differentiation using time-resolved autofluorescence spectroscopy. *Gastrointest. Endosc.* 48:390–394, 1998.
[86]Naghavi, M., P. Libby, E. Falk, S. W. Casscells, S. Litovsky, J. Rumberger, J. J. Badimon, C. Stefanadis, P. Moreno, G. Pasterkamp, Z. Fayad, P. H. Stone, S. Waxman, P. Raggi, M. Madjid, A. Zarrabi, A. Burke, C. Yuan, P. J. Fitzgerald, D. S. Siscovick, C. L. de Korte, M. Aikawa, K. E. Juhani Airaksinen, G. Assmann, C. R. Becker, J. H. Chesebro, A. Farb, Z. S. Galis, C. Jackson, I. K. Jang, W. Koenig, R. A. Lodder, K. March, J. Demirovic, M. Navab, S. G. Priori, M. D. Rekhter, R. Bahr, S. M. Grundy, R. Mehran, A. Colombo, E. Boerwinkle, C. Ballantyne, W. Insull, Jr., R. S. Schwartz, R. Vogel, P. W. Serruys, G. K. Hansson, D. P. Faxon, S. Kaul, H. Drexler, P. Greenland, J. E. Muller, R. Virmani, P. M. Ridker, D. P. Zipes, P. K. Shah, and J. T. Willerson. From vulnerable plaque to vulnerable patient: a call for new definitions and risk assessment strategies: Part I. *Circulation* 108:1664–1672, 2003.
[87]Nordstrom, R. J., L. Burke, J. M. Niloff, and J. F. Myrtle. Identification of cervical intraepithelial neoplasia (CIN) using UV-excited fluorescence and diffuse-reflectance tissue spectroscopy. *Lasers Surg. Med.* 29:118–127, 2001.
[88]O' Connor, D. V., W. R. Ware, and J. C. Andre. Deconvolution of fluorescence decay curves—critical comparison of techniques. *J. Phys. Chem.* 83:1333–1343, 1979.
[89]Panjehpour, M., C. E. Julius, M. N. Phan, T. Vo-Dinh, and S. Overholt. Laser-induced fluorescence spectroscopy for in vivo diagnosis of non-melanoma skin cancers. *Lasers Surg. Med.* 31:367–373, 2002.
[90]Pavlova, I., C. R. Weber, R. A. Schwarz, M. Williams, A. El-Naggar, A. Gillenwater, and R. Richards-Kortum. Monte Carlo model to describe depth selective fluorescence spectra of epithelial tissue: applications for diagnosis of oral precancer. *J. Biomed. Opt.* 13:064012, 2008.
[91]Pavlova, I., C. R. Weber, R. A. Schwarz, M. D. Williams, A. M. Gillenwater, and R. Richards-Kortum. Fluorescence spectroscopy of oral tissue: Monte Carlo modeling with site-specific tissue properties. *J. Biomed. Opt.* 14:014009, 2009.
[92]Pfefer, T. J., D. Y. Paithankar, J. M. Poneros, K. T. Schomacker, and N. S. Nishioka. Temporally and spectrally resolved fluorescence spectroscopy for the detection of high grade dysplasia in Barrett's esophagus. *Lasers Surg. Med.* 32:10–16, 2003.

[93]Phipps, J. E., N. Hatami, Z. S. Galis, J. D. Baker, M. C. Fishbein, and L. Marcu. A fluorescence lifetime spectroscopy study of matrix metalloproteinases-2 and -9 in human atherosclerotic plaque. *J. Biophotonics* 4:650–658, 2011.
[94]Pitts, D. J., and M.-A. Mycek. Design and development of a rapid acquisition laser-based fluorometer with simultaneous spectral and temporal resolution. *Rev. Sci. Instrum.* 72:3061–3072, 2001.
[95]Pogue, B. W., S. Gibbs-Strauss, P. A. Valdes, K. Samkoe, D. W. Roberts, and K. D. Paulsen. Review of Neurosurgical Fluorescence Imaging methodologies. *IEEE J. Sel. Top. Quantum Electron.* 16:493–505, 2010.
[96]Rajaram, N., J. S. Reichenberg, M. R. Migden, T. H. Nguyen, and J. W. Tunnell. Pilot clinical study for quantitative spectral diagnosis of non-melanoma skin cancer. *Lasers Surg. Med.* 42:716–727, 2010.
[97]Ramanujam, N. Fluorescence spectroscopy of neoplastic and non-neoplastic tissues. *Neoplasia* 2:89–117, 2000.
[98]Redden Weber, C., R. A. Schwarz, E. N. Atkinson, D. D. Cox, C. Macaulay, M. Follen, and R. Richards-Kortum. Model-based analysis of reflectance and fluorescence spectra for in vivo detection of cervical dysplasia and cancer. *J. Biomed. Opt.* 13:064016, 2008.
[99]Richards-Kortum, R., and E. Sevick-Muraca. Quantitative optical spectroscopy for tissue diagnosis. *Annu. Rev. Phys. Chem.* 47:555–606, 1996.
[100]Roberts, M. S., Y. Dancik, T. W. Prow, C. A. Thorling, L. L. Lin, J. E. Grice, T. A. Robertson, K. Konig, and W. Becker. Non-invasive imaging of skin physiology and percutaneous penetration using fluorescence spectral and lifetime imaging with multiphoton and confocal microscopy. *Eur. J. Pharm. Biopharm.* 77:469–488, 2011.
[101]Roblyer, D., C. Kurachi, V. Stepanek, M. D. Williams, A. K. El-Naggar, J. J. Lee, A. M. Gillenwater, and R. Richards-Kortum. Objective detection and delineation of oral neoplasia using autofluorescence imaging. *Cancer Prev. Res. (Phila.)* 2:423–431, 2009.
[102]Roblyer, D., R. Richards-Kortum, K. Sokolov, A. K. El-Naggar, M. D. Williams, C. Kurachi, and A. M. Gillenwater. Multispectral optical imaging device for in vivo detection of oral neoplasia. *J. Biomed. Opt.* 13:024019, 2008.
[103]Rydell, R., C. Eker, S. Andersson-Engels, A. Krogdahl, P. Wahlberg, and K. Svanberg. Fluorescence investigations to classify malignant laryngeal lesions in vivo. *Head Neck* 30:419–426, 2008.
[104]Scepanovic, O. R., M. Fitzmaurice, A. Miller, C. R. Kong, Z. Volynskaya, R. R. Dasari, J. R. Kramer, and M. S. Feld. Multimodal spectroscopy detects features of vulnerable atherosclerotic plaque. *J. Biomed. Opt.* 16:011009, 2011.
[105]Schwarz, R. A., W. Gao, D. Daye, M. D. Williams, R. Richards-Kortum, and A. M. Gillenwater. Autofluorescence and diffuse reflectance spectroscopy of oral epithelial tissue using a depth-sensitive fiber-optic probe. *Appl. Opt.* 47:825–834, 2008.
[106]Schwarz, R. A., W. Gao, C. Redden Weber, C. Kurachi, J. J. Lee, A. K. El-Naggar, R. Richards-Kortum, and A. M. Gillenwater. Noninvasive evaluation of oral lesions using depth-sensitive optical spectroscopy. *Cancer* 115:1669–1679, 2009.
[107]Schweitzer, D., M. Hammer, F. Schweitzer, R. Anders, T. Doebbecke, S. Schenke, E. R. Gaillard, and E. R. Gaillard. In vivo measurement of time-resolved autofluorescence at the human fundus. *J. Biomed. Opt.* 9:1214–1222, 2004.
[108]Schweitzer, D., S. Quick, M. Klemm, M. Hammer, S. Jentsch, and J. Dawczynski. Time-resolved autofluorescence in retinal vascular occlusions. *Ophthalmologe* 107:1145–1152, 2010.
[109]Schweitzer, D., S. Quick, S. Schenke, M. Klemm, S. Gehlert, M. Hammer, S. Jentsch, and J. Fischer. Comparison of parameters of time-resolved autofluorescence between healthy subjects and patients suffering from early AMD. *Ophthalmologe* 106:714–722, 2009.
[110]Sevick-Muraca, E. M., R. Sharma, J. C. Rasmussen, M. V. Marshall, J. A. Wendt, H. Q. Pham, E. Bonefas, J. P. Houston, L. Sampath, K. E. Adams, D. K. Blanchard, R. E. Fisher, S. B. Chiang, R. Elledge, and M. E. Mawad. Imaging of lymph flow in breast cancer patients after microdose administration of a near-infrared fluorophore: feasibility study. *Radiology* 246:734–741, 2008.
[111]Sun, Y., A. J. Chaudhari, M. Lam, H. Xie, D. R. Yankelevich, J. Phipps, J. Liu, M. C. Fishbein, J. M. Cannata, K. K. Shung, and L. Marcu. Multimodal characterization of compositional, structural and functional features of human atherosclerotic plaques. *Biomed. Opt. Expres.* 2:2288–2298, 2011.
[112]Sun, Y., N. Hatami, M. Yee, J. Phipps, D. S. Elson, F. Gorin, R. J. Schrot, and L. Marcu. Fluorescence lifetime imaging microscopy for brain tumor image-guided surgery. *J. Biomed. Opt.* 15:056022, 2010.
[113]Sun, Y., J. Park, D. N. Stephens, J. A. Jo, L. Sun, J. M. Cannata, R. M. Saroufeem, K. K. Shung, and L. Marcu. Development of a dual-modal tissue diagnostic system combining time-resolved fluorescence spectroscopy and ultrasonic backscatter microscopy. *Rev. Sci. Instrum.* 80:065104, 2009.
[114]Sun, Y., J. Phipps, D. S. Elson, H. Stoy, S. Tinling, J. Meier, B. Poirier, F. S. Chuang, D. G. Farwell, and L. Marcu. Fluorescence lifetime imaging microscopy: in vivo application to diagnosis of oral carcinoma. *Opt. Lett.* 34:2081–2083, 2009.
[115]Sun, Y., Y. Sun, D. Stephens, H. Xie, J. Phipps, R. Saroufeem, J. Southard, D. S. Elson, and L. Marcu. Dynamic tissue analysis using time- and wavelength-resolved fluorescence spectroscopy for atherosclerosis diagnosis. *Opt. Express* 19:3890–3901, 2011.
[116]Sun, Y., J. Meier, N. Hatami, J. Phipps, R. J. Schrot, B. Poirier, G. Farwell, D. Elson, and L. Marcu. Fluorescence Lifetime Imaging Microscopy (FLIM) for intraoperative tumor delineation: a study in patients. *BODA*, 2011.
[117]Suzuki, H., Y. Saito, H. Ikehara, and I. Oda. Evaluation of visualization of squamous cell carcinoma of esophagus and pharynx using an autofluorescence imaging videoendoscope system. *J. Gastroenterol. Hepatol.* 24:1834–1839, 2009.
[118]Thekkek, N., and R. Richards-Kortum. Optical imaging for cervical cancer detection: solutions for a continuing global problem. *Nat. Rev. Cancer* 8:725–731, 2008.
[119]Thiberville, L., M. Salaun, S. Lachkar, S. Dominique, S. Moreno-Swirc, C. Vever-Bizet, and G. Bourg-Heckly. Human in vivo fluorescence microimaging of the alveolar ducts and sacs during bronchoscopy. *Eur. Respir. J.* 33:974–985, 2009.
[120]Toms, S. A., W. C. Lin, R. J. Weil, M. D. Johnson, E. D. Jansen, and A. Mahadevan-Jansen. Intraoperative optical spectroscopy identifies infiltrating glioma margins with high sensitivity. *Neurosurgery* 61:327–335; discussion 335–336, 2007.

[121]Udenfriend, S., 1969. Fluorescence assay in biology and medicine. In: Molecular Biology, edited by R. Consden. London: Academic Press, I and II 1969, pp. 517–660.
[122]Uehlinger, P., T. Gabrecht, T. Glanzmann, J. P. Ballini, A. Radu, S. Andrejevic, P. Monnier, and G. Wagnieres. In vivo time-resolved spectroscopy of the human bronchial early cancer autofluorescence. *J. Biomed. Opt*. 14:024011, 2009.
[123]Utzinger, U., and R. R. Richards-Kortum. Fiber optic probes for biomedical optical spectroscopy. *J. Biomed. Opt*. 8:121–147, 2003.
[124]Vedeswari, C. P., S. Jayachandran, and S. Ganesan. In vivo autofluorescence characteristics of pre- and post-treated oral submucous fibrosis: a pilot study. *Indian J. Dent. Res*. 20:261–267, 2009.
[125]Wagnieres, G. A., W. M. Star, and B. C. Wilson. In vivo fluorescence spectroscopy and imaging for oncological applications. *Photochem. Photobiol*. 68:603–632, 1998.
[126]Ware, W. R., L. J. Doemeny, and T. L. Nemzek. Deconvolution of Fluorescence and Phosphorescence Decay Curves - Least-Squares Method. *J. Phy. Chem*. 77:2038–2048, 1973.
[127]Wilson, B. C. Detection and treatment of dysplasia in Barrett's esophagus: a pivotal challenge in translating biophotonics from bench to bedside. *J. Biomed. Opt*. 12:051401, 2007.
[128]www.novadaq.com/. Accessed December 30, 2011.
[129]www.karlstorz.com/. Accessed December 30, 2011.
[130]www.pentaxmedical.com/. Accessed December 30, 2011.
[131]www.richardwolfusa.com/. Accessed December 30, 2011.
[132]www.guidedinc.com/. Accessed December 30, 2011.
[133]www.velscope.com/. Accessed December 30, 2011.
[134]www.jenlab.de/DermaInspect-R.29.0.html. Accessed December 30, 2011.
[135]www.picoquant.com/. Accessed December 30, 2011.
[136]www.becker-hickl.de/. Accessed December 30, 2011.
[137]Zellweger, M., D. Goujon, R. Conde, M. Forrer, H. van den Bergh, and G. Wagnieres. Absolute autofluorescence spectra of human healthy, metaplastic, and early cancerous bronchial tissue in vivo. *Appl. Opt*. 40:3784–3791, 2001.
[138]Zellweger, M., P. Grosjean, D. Goujon, P. Monnier, H. van den Bergh, and G. Wagnieres. In vivo autofluorescence spectroscopy of human bronchial tissue to optimize the detection and imaging of early cancers. *J. Biomed. Opt*. 6:41–51, 2001.
[139]Zhu, C., E. S. Burnside, G. A. Sisney, L. R. Salkowski, J. M. Harter, B. Yu, and N. Ramanujam. Fluorescence spectroscopy: an adjunct diagnostic tool to image-guided core needle biopsy of the breast. *IEEE Trans. Biomed. Eng*. 56:2518–2528, 2009.
[140]Zipfel, W. R., R. M. Williams, R. Christie, A. Y. Nikitin, B. T. Hyman, and W. W. Webb. Live tissue intrinsic emission microscopy using multiphoton-excited native fluorescence and second harmonic generation. *Proc. Natl. Acad. Sci. USA* 100:7075–7080, 2003.